Semisynthetic guanidino lipoglycopeptides with potent in vitro and in vivo antibacterial activity

Groesen, E. van; Mons, E.; Kotsogianni, A.I.; Arts, M.; Tehrani, K.H.M.E.; Wade, N.; ... ; Martin, N.I.

ANTIBIOTICS

Semisynthetic guanidino lipoglycopeptides with potent in vitro and in vivo antibacterial activity

Emma van Groesen[1]†, Elma Mons[1]†, Ioli Kotsogianni[1], Melina Arts[2], Kamaleddin H. M. E. Tehrani[1], Nicola Wade[1], Vladyslav Lysenko[1], Florence M. Stel[1], Jordy T. Zwerus[1], Stefania De Benedetti[2], Alexander Bakker[3], Parichita Chakraborty[4], Mario van der Stelt[3], Dirk-Jan Scheffers[4], Jairo Gooskens[5], Wiep Klaas Smits[6], Kirsty Holden[7], Peter S. Gilmour[8], Joost Willemse[9], Christopher A. Hitchcock[10], J. G. Coen van Hasselt[11], Tanja Schneider[2], Nathaniel I. Martin[1]*

Gram-positive bacterial infections present a major clinical challenge, with methicillin- and vancomycin-resistant strains continuing to be a cause for concern. In recent years, semisynthetic vancomycin derivatives have been developed to overcome this problem as exemplified by the clinically used telavancin, which exhibits increased antibacterial potency but has also raised toxicity concerns. Thus, glycopeptide antibiotics with enhanced antibacterial activities and improved safety profiles are still necessary. We describe the development of a class of highly potent semisynthetic glycopeptide antibiotics, the guanidino lipoglycopeptides, which contain a positively charged guanidino moiety bearing a variable lipid group. These glycopeptides exhibited enhanced in vitro activity against a panel of Gram-positive bacteria including clinically relevant methicillin-resistant *Staphylococcus aureus* (MRSA) and vancomycin-resistant strains, showed minimal toxicity toward eukaryotic cells, and had a low propensity for resistance selection. Mechanistically, guanidino lipoglycopeptides engaged with bacterial cell wall precursor lipid II with a higher binding affinity than vancomycin. Binding to both wild-type D-Ala-D-Ala lipid II and the vancomycin-resistant D-Ala-D-Lac variant was confirmed, providing insight into the enhanced activity of guanidino lipoglycopeptides against vancomycin-resistant isolates. The in vivo efficacy of guanidino lipoglycopeptide EVG7 was evaluated in a *S. aureus* murine thigh infection model and a 7-day sepsis survival study, both of which demonstrated superiority to vancomycin. Moreover, the minimal to mild kidney effects at suprathera-peutic doses of EVG7 indicate an improved therapeutic safety profile compared with vancomycin. These findings position guanidino lipoglycopeptides as candidates for further development as antibacterial agents for the treatment of clinically relevant multidrug-resistant Gram-positive infections.

INTRODUCTION

Antimicrobial resistance poses a major threat to human health and is driven by the rise in multidrug-resistant bacteria coupled with the steep decrease in antibiotic drug discovery (*1*, *2*). Infections with Gram-positive pathogens such as methicillin-resistant *Staphylococcus aureus* (MRSA) are increasingly responsible for both community- and hospital-acquired infections that result in substantial morbidity and mortality (*1*–*4*). For decades, the glycopeptide antibiotic vancomycin (1, fig. S1) has been used to effectively treat infections due to MRSA and other Gram-positive pathogens. In recent years, however, a variety of vancomycin-resistant clinical isolates have been reported. These strains include vancomycin-intermediate *S. aureus* (VISA), with a minimum inhibitory concentration (MIC) of 4 to 8 μg/ml; heteroresistant VISA, which is largely susceptible with a subpopulation of resistant species; and vancomycin-resistant *S. aureus* (VRSA), with an MIC of ≥16 μg/ml (*3*, *4*). Also of note are organisms that exhibit moderate reductions in vancomycin susceptibility (increased MIC from ≤1 to 1.5 to 2 μg/ml), a phenomenon known as MIC creep, for which the associated impact on clinical outcomes remains a topic of debate (*4*, *5*). In addition to the increasing difficulties faced in treating *S. aureus* infections, vancomycin-resistant enterococci (VRE) have emerged as a serious clinical challenge against which vancomycin is of no use. It is now estimated that 30% of all health care–associated enterococcal infections are resistant to vancomycin (*2*). As noted in a 2019 US Centers for Disease Control and Prevention (CDC) report, infections due to MRSA and VRE total nearly 400,000 per year and account for half of all antimicrobial resistance–associated deaths in the United States (*2*). In Europe, MRSA and VRE cause approximately 170,000 infections annually and are implicated in 25% of antimicrobial resistance-related deaths (*6*). In more recent studies, antimicrobial resistance accounted for 1.27 million deaths worldwide in 2019, with drug-resistant Gram-positive species *S. aureus* and *Streptococcus pneumoniae* alone being responsible for a combined 0.5 million annual deaths (*7*).

In susceptible strains, vancomycin targets the cell wall precursor lipid II by binding to the D-Ala-D-Ala terminus of the pentapeptide by a defined network of five hydrogen bonds. This interaction effectively sequesters lipid II and prevents it from being further

[1]Biological Chemistry Group, Institute of Biology Leiden, Leiden University, 2300 RA Leiden, Netherlands. [2]Institute for Pharmaceutical Microbiology, University Hospital Bonn, University of Bonn, 53113 Bonn, Germany. [3]Department of Molecular Physiology, Leiden Institute of Chemistry, Leiden University, 2300 RA Leiden, Netherlands. [4]Department of Molecular Microbiology, Groningen Biomolecular Sciences and Biotechnology Institute, University of Groningen, 9700 AB Groningen, Netherlands. [5]Department of Medical Microbiology, Leiden University Center for Infectious Diseases (LUCID), Leiden University Medical Center, 2333 ZA Leiden, Netherlands. [6]Experimental Bacteriology, Leiden University Center for Infectious Diseases (LUCID), Leiden University Medical Center, 2333 ZA Leiden, Netherlands. [7]Evotec (U.K.) Ltd., Alderley Park, Macclesfield, Cheshire, SK10 4TG UK. [8]The Drug Development Team, 2321 DK Leiden, Netherlands. [9]Institute of Biology Leiden, Leiden University, 2300 RA Leiden, Netherlands. [10]6 Carnoustie Close, Molehill Road, Chestfield, Whitstable, Kent CT5 3PW, UK. [11]Division of Systems Biomedicine and Pharmacology, Leiden Academic Centre for Drug Research, Leiden University, 2300 RA Leiden, Netherlands.
*Corresponding author. Email: n.i.martin@biology.leidenuniv.nl
†These authors contributed equally to this work.

incorporated into the growing peptidoglycan by bacterial transpeptidases and transglycosylases, which in turn leads to inhibition of cell wall biosynthesis. This interference with peptidoglycan polymerization results in compromised bacterial cell wall integrity and subsequent cell lysis (*8*–*11*). High resistance to vancomycin is achieved by target modification, wherein the D-Ala-D-Ala termini of peptidoglycan intermediates are mutated to D-Ala-D-Lac/Ser. The introduction of the corresponding depsipeptide motif in D-Ala-D-Lac mutants results in loss of one hydrogen bond and repulsive electrostatic interactions, which are associated with a >1000-fold reduction in binding affinity, rendering vancomycin ineffective (*12*, *13*). Resistance to vancomycin is predominantly due to acquisition of the *vanA* and *vanB* gene clusters leading to D-Ala-D-Lac incorporation (*14*, *15*). However, reduced vancomycin susceptibility can also occur in the absence of a dedicated gene cluster. Such vancomycin-intermediate and vancomycin-resistant strains are instead characterized by a thickened cell wall and decreased autolytic activity, leading to an increased abundance of D-Ala-D-Ala motifs that effectively trap vancomycin, thereby allowing for continued growth of the peptidoglycan layer (*4*, *8*, *16*, *17*).

In response to the rise of vancomycin resistance, the lipopeptide daptomycin and the oxazolidinone linezolid were both introduced to the clinic in the early 2000s. However, strains of MRSA and VRE resistant to both antibiotics arose shortly thereafter (*18*–*21*). In parallel, next-generation glycopeptide antibiotics were actively pursued, starting with the natural product teicoplanin (2) (fig. S1), which was approved for use in Europe in 1998 but is not used in the North American market (*11*). The structure of teicoplanin differs from that of vancomycin, most notably because of the presence of a hydrophobic acyl tail that is associated with its enhanced antibacterial activity. This in turn spawned interest in semisynthetic lipoglycopeptides, including telavancin (3), dalbavancin (4), and oritavancin (5) (fig. S1), which were all subsequently developed and approved for clinical use between 2009 and 2014 (*11*). Although these semisynthetic glycopeptides exhibit more potent antibiotic activity than vancomycin, telavancin was recently issued a black-box warning from the US Food and Drug Administration because of its associated toxicity concerns (*22*). In addition, dalbavancin and oritavancin display unusual pharmacokinetic (PK) properties with half-lives of multiple days, allowing for once-weekly dosing (*23*). Furthermore, these semisynthetic lipoglycopeptides are known to have poor aqueous solubility (*24*, *25*), a practical yet important characteristic for clinically used agents. Therefore, the development of glycopeptide antibiotics with improved antibacterial activity and PK and safety profiles continues to be of great importance (*26*).

Strategies have been described in recent years for pursuing glycopeptide antibiotics with enhanced properties (*11*, *27*–*47*), ranging from total synthesis approaches aimed at vancomycin backbone modification to overcome resistance (*40*–*46*) to semisynthetic strategies typically involving the introduction of positively charged motifs or hydrophobic moieties (*29*–*40*) as well as antibiotic hybrids (*27*–*29*). In particular, the addition of positively charged functional groups to vancomycin to improve antibacterial activity has been described (*31*–*34*). Given our previous synthesis of biologically active compounds containing substituted guanidine groups (*48*–*51*), we hypothesized that the introduction of a guanidinium motif at the vancosamine site in vancomycin might provide semisynthetic glycopeptides with enhanced properties. Here, we report the development of guanidino lipoglycopeptides, a promising class of semisynthetic vancomycin derivatives containing lipidated guanidine moieties that show activity against a variety of Gram-positive bacteria in vitro as well as in vivo, with low propensity for resistance and favorable toxicity profiles.

RESULTS

Design, synthesis, and in vitro evaluation of guanidino lipoglycopeptides

The synthetic route devised for the preparation of guanidino lipoglycopeptides relies on selective modification of the vancosamine nitrogen in vancomycin by reductive amination (fig. S2), which is known to be an effective means of modifying this site (*11*, *31*). The aldehyde building blocks required to introduce the lipidated guanidine moiety were prepared using a robust and modular building block approach. Specifically, the lipidated guanidino group was prepared as the corresponding Alloc-carbamate protected species and linked to an aromatic aldehyde providing the reactive handle for the reductive amination step. After subsequent Alloc group removal, the guanidino lipoglycopeptides were purified by high-performance liquid chromatography (HPLC). In this way, guanidino lipoglycopeptides EVG6 to EVG20 were prepared incorporating a diverse panel of lipid tails, including linear, branched, unsaturated, aromatic lipids (Fig. 1). Representative chemical characterization of EVG7 is provided in fig. S3 and tables S1 and S2.

Antibacterial activities of EVG6 to EVG20 were assessed in broth microdilution assays (Table 1). Growth medium was supplemented with 0.002% polysorbate 80 (P80), as recommended for clinical lipoglycopeptide antibiotics (such as dalbavancin and oritavancin) (*52*–*54*). MICs determined in the absence of P80 confirmed the need for P80 supplementation (table S3). Most compounds were highly effective against an initial panel of Gram-positive pathogens, with activities superior to vancomycin and other clinically used glycopeptide antibiotics. The most potent compounds were >100-fold more active than vancomycin against methicillin-sensitive *S. aureus* (MSSA) and MRSA and even ≥1000-fold more active against VISA. Furthermore, against MRSA and VISA, the most active guanidino lipoglycopeptides exhibited MICs >8-fold and >30-fold lower than those observed for the most potent clinically used glycopeptides (oritavancin and telavancin, respectively). In addition, most candidates were ≥100-fold more active than vancomycin against VRSA, with some showing enhancements as high as 2000-fold. In the case of VRE with the VanA phenotype, the compounds showed increased potencies of up to 1000-fold compared with vancomycin and as high as 16,000-fold against VanB-type VRE isolates. In addition, the most potent guanidino lipoglycopeptides were >50-fold more active than vancomycin against vancomycin-sensitive enterococci (VSE) and *S. pneumoniae*. Candidate compounds were further assessed against a broader panel of MRSA, VISA, VRSA, and VRE (*Enterococcus faecalis)* strains, again demonstrating superior activity relative to vancomycin and equipotent or superior activity to the other clinically relevant glycopeptides (table S4). Six of the most potent candidates (EVG7, EVG8, EVG9, EVG14, EVG16, and EVG18) were selected for further assessment against 30 different VRE isolates, revealing MIC_{50} and MIC_{90} values ranging from 0.031 to 1.0 and 0.5 to 8.0 μg/ml, respectively (table S5). EVG7, EVG14, and EVG18 were further evaluated against a panel of 30 genetically diverse MRSA and BORSA (borderline oxacillin-resistant *S. aureus*) clinical isolates, including several LA-MRSA

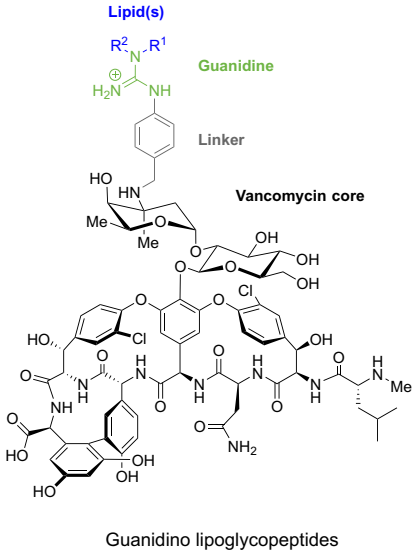

Compound	R^1	R^2
EVG6	*n*-C_6H_{13}	H
EVG7	*n*-C_7H_{15}	H
EVG8	*n*-C_8H_{17}	H
EVG9	*n*-C_9H_{19}	H
EVG10	*n*-$C_{10}H_{21}$	H
EVG11	*n*-$C_{12}H_{25}$	H
EVG12	*n*-$C_{14}H_{29}$	H
EVG13	*n*-C_4H_9	*n*-C_4H_9
EVG14	*n*-C_6H_{13}	*n*-C_6H_{13}
EVG15	*n*-$C_{10}H_{21}$	*n*-$C_{10}H_{21}$
EVG16	Ger	H
EVG17	Far	H
EVG18	CH_2-CBP	H
EVG19	TCD	H
EVG20	CH_2-TCD	H

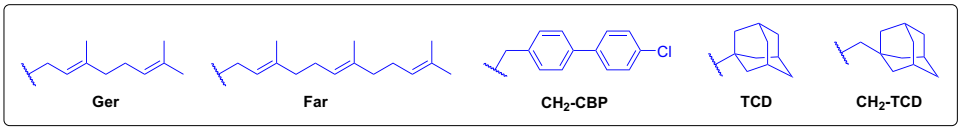

Fig. 1. Structures of guanidino lipoglycopeptides EVG6 to EVG20 prepared in the present study. Guanidine moiety (green) and the various lipid tails (blue) are shown.

(livestock-associated MRSA) and HO-MRSA (hospital-onset MRSA) strains (table S6). We consistently found that guanidino lipoglycopeptides had superior activity (MIC_{90} = 0.031 to 0.063 μg/ml) to vancomycin (MIC_{90} = 1 μg/ml) and equipotent activity to dalbavancin (MIC_{90} = 0.031 to 0.063 μg/ml). Against an expanded panel of VISA and VRSA strains, EVG7, EVG14, and EVG18 were consistently more active than vancomycin and equipotent or superior to telavancin (table S7). Similarly to all clinically used glycopeptides, the guanidino lipoglycopeptides exhibited no activity against Gram-negative bacteria (table S8).

Structure-activity relationship

The results of the MIC assays indicate that guanidino lipoglycopeptides are highly active with marked enhancements in activity relative to vancomycin (Table 1 and tables S4 to S7). Analogs containing straight chain aliphatic lipid tails comprising seven to nine carbon atoms, as in EVG7 to EVG9 (heptyl-nonyl) were more potent against MRSA, VISA, and vanB-type VRE strains, whereas the introduction of longer lipid tails, such as for EVG10 and EVG11 (decyl, dodecyl) performed better against VanA-type VRSA and VRE. However, when the lipids became longer, such as for EVG12 (tetradecyl), activity was compromised, as reflected by reduced potency against MSSA and MRSA. Conversely, the inclusion of shorter lipids, as in analog EVG6 (hexyl), resulted in a reduction in activity against vancomycin-resistant strains. Thus, among the monosubstituted guanidino lipoglycopeptides, optimal potency appears to be achieved by incorporation of a linear lipid moiety of 7 to 12 carbon atoms. We also examined the effect of including two lipid tails on the guanidino moiety, as in compounds EVG13 to EVG15. Here, a slightly different trend was observed compared with the monosubstituted guanidino lipoglycopeptides: Whereas the C_{10} monosubstituted EVG10 was more active than the C_6 monosubstituted EVG6, the trend was reversed for the bis-substituted analogs. In this case, the C_6 bis-lipidated EVG14 was much more potent than the C_{10} bis-lipidated EVG15, with the latter also having reduced activity compared with vancomycin. In addition to mono- and bis-substitution with linear aliphatic lipids, we explored the introduction of more exotic lipids including branched, unsaturated, aromatic, and adamantyl-based substituents (compounds EVG16 to EVG20). In general, these analogs were also highly active, with EVG16 to EVG18 performing particularly well against vancomycin-resistant strains.

Serum reversal and hemolytic activity

The activity of compounds containing large hydrophobic groups can be affected by nonspecific interactions with serum proteins (*55*, *56*). Thus, we examined the antibiotic activity of guanidino lipoglycopeptides in the presence of 50% sheep serum (Table 1). Clinically used lipoglycopeptides 2 to 5 all had a four- to eightfold reduction in activity in the presence of serum, whereas the same was not observed for guanidino lipoglycopeptides. For compounds EVG6, EVG7, EVG10, EVG11, EVG13, EVG14, EVG16, and EVG18, little to no change in antibacterial activity was observed upon addition of serum to the media. For other compounds, addition of serum affected activity, although not in a manner indicating a specific trend: EVG8 and EVG9, bearing linear C_8 and C_9 lipids, respectively, showed eightfold reduction in activity in the presence of serum, whereas MIC values of EVG10 and EVG11, bearing linear C_{10} and C_{11} lipids, were only increased by a factor of two. For EVG16 to EVG20 containing structurally more diverse lipids, the farnesylated compound EVG17 experienced a 16-fold reduction of activity in the presence of serum, whereas EVG16 and EVG18 to EVG20 experienced only 2- to 4-fold increases in MIC.

The capacity of guanidino lipoglycopeptides to lyse erythrocytes was evaluated to assess general membrane disruptive properties (Table 1). Most guanidino lipoglycopeptides exhibited minimal hemolytic activity when tested up to 1000-fold MIC (MIC values based on activity against MRSA). Derivatives with shorter lipids (EVG6, EVG7, EVG13, and EVG19) induced little to no hemolysis at the highest concentrations tested (64 μg/ml), whereas clinically used oritavancin caused 53% hemolysis at the same concentration (table S9). Likewise, a number of guanidino lipoglycopeptides containing large hydrophobic groups (EVG10 to EVG12, EVG15, EVG17, and EVG18) caused hemolysis similar to oritavancin at 64 μg/ml (table S9).

Microbiological characterization

Building on the above findings, the guanidino lipoglycopeptides EVG7 and EVG18 were taken forward for further evaluation. Time-kill kinetics of these compounds against VanA-type VRE (Fig. 2A)

Table 1. In vitro antibacterial activity against Gram-positive strains and hemolytic activity. N.D., not determined; Ger, geranyl; Far, farnesyl; CBP, 4-chloro-1,1′-biphenyl; TCD, tricyclo[3.3.1.13,7]decane or adamantane.

		MIC (μg/ml)*									Hemolysis (%)†	
		MSSA	MRSA	MRSA‡ +50% serum	VISA	VRSA	VSE	VRE (VanA)	VRE (VanB)	VSSP	100× MIC	1000× MIC
Clinical (lipo)glycopeptide antibiotics												
Vancomycin (1)		1	1	0.25	8	>128	0.5	>128	128	0.5	<1	<1
Teicoplanin (2)		0.5	0.5	2	16	32	0.5	>128	0.25	0.031	<1	<1
Telavancin (3)		0.125	0.125	1	0.25	4	0.016	4	≤0.008	≤0.008	<1	<1
Dalbavancin (4)		0.063	0.063	2	1	16	0.063	64	0.016	≤0.008	<1	<1
Oritavancin (5)		0.25	0.063	0.25	1	0.25	0.063	0.5	0.125	≤0.008	1.6 ± 0.16	48 ± 4.8
Guanidino lipoglycopeptides												
EVG6	-C_6H_{13}	0.063	0.063	0.063	0.25	4	0.031	8	0.031	0.016	<1	<1
EVG7	-C_7H_{15}	≤0.008	0.016	0.031	0.031	1	≤0.008	2	≤0.008	≤0.008	<1	<1
EVG8	-C_8H_{17}	≤0.008	≤0.008	0.063	≤0.008	0.5	0.016	1	≤0.008	≤0.008	<1	<1
EVG9	-C_9H_{19}	0.016	≤0.008	0.063	≤0.008	0.125	0.031	0.5	≤0.008	≤0.008	<1	7.5 ± 7.5
EVG10	-$C_{10}H_{21}$	0.016	0.063	0.125	0.016	0.063	0.016	0.25	≤0.008	≤0.008	2.8 ± 0.059	45 ± 0.83
EVG11	-$C_{12}H_{25}$	0.125	0.5	1	0.5	0.125	0.125	0.125	0.031	≤0.008	40 ± 1.4	96 ± 1.5
EVG12	-$C_{14}H_{29}$	2	4	16	4	0.5	0.5	0.5	0.5	0.031	92 ± 2.7	N.D.
EVG13	(-C_4H_9)$_2$	0.125	0.125	0.063	0.5	16	0.063	32	0.5	0.063	<1	<1
EVG14	(-C_6H_{13})$_2$	≤0.008	0.063	0.063	≤0.008	0.25	≤0.008	1	≤0.008	≤0.008	<1	9.1 ± 1.1
EVG15	(-$C_{10}H_{21}$)$_2$	16	16	64	32	8	4	8	4	2	74 ± 0.48	N.D.
EVG16	-Ger	≤0.008	0.031	0.063	≤0.008	0.063	≤0.008	1	≤0.008	≤0.008	<1	3.4 ± 0.50
EVG17	-Far	0.031	0.063	1	0.125	0.125	0.031	0.125	0.016	≤0.008	2.8 ± 0.049	50 ± 0.99
EVG18	-CH_2-CBP	0.016	0.031	0.063	0.016	0.063	≤0.008	0.125	≤0.008	≤0.008	<1	13 ± 0.20
EVG19	-TCD	0.016	0.031	0.125	0.125	8	≤0.008	8	0.016	0.016	<1	<1
EVG20	-CH_2-TCD	≤0.008	≤0.008	0.031	0.016	2	≤0.008	2	≤0.008	≤0.008	<1	<1

*MIC determined by broth microdilution assay in tryptic soy broth (TSB) supplemented with 0.002% P80. MIC values represent the median of a minimum of triplicates. MIC, MIC_{50}, and MIC_{90} values on extended panel of strains are in tables S4 to S7. Bacterial strains: MSSA ATCC29213; MRSA USA300; VISA NRS36 (LIM 2); VRSA VRS3b (HIP 13419); VSE (vancomycin-sensitive *E. faecium*) E980; VRE (VanA) (vancomycin-resistant *E. faecium*) E155; VRE (VanB) (vancomycin-resistant *E. faecium*) E7314; and VSSP (vancomycin-sensitive *S. pneumoniae*) 153 (ATCC6305). †Hemolysis of sheep erythrocytes after incubation with antibiotic at concentrations 100- and 1000-fold above the respective MICs for MRSA USA300. Data are mean ± SD of a minimum of triplicates. ‡Serum reversal MIC for growth inhibition of MRSA USA300 in the presence of 50% sheep serum.

and MRSA (fig. S4) were evaluated in comparison with clinically used vancomycin, telavancin, and daptomycin. The guanidino lipoglycopeptides had a slow bactericidal effect against VRE and MRSA, similar to vancomycin and telavancin. Time-kill data confirmed the results of the broth microdilution assays (Table 1), with lower concentrations of guanidino lipoglycopeptides being required to achieve the same reduction in bacterial titer as clinically used glycopeptide antibiotics. In addition, EVG7 showed superior activity compared with daptomycin, commonly used to treat MRSA infections. Although daptomycin (5 μg/ml) administration led to an initial drop in MRSA colony-forming units (CFU), a high bacterial titer was again present 24 hours later (fig. S4). By comparison, no colonies were detected after 24 hours when the more potent EVG7 was used (at 0.156 μg/ml). To characterize the pharmacodynamic characteristics of EVG7, we performed extensive time-kill studies with vancomycin as comparator using two MSSA and MRSA luminescent reporter strains (*57*, *58*) for a wide range of concentrations and time points (fig. S5), finding an approximately fivefold increased slope and a twofold reduced median effective concentration for EVG7 in comparison with vancomycin, with negligible differences in the maximum drug effect parameter. A steep slope indicates that there is a more extensive increase in bacterial killing as antibiotic concentrations are increased, in line with antibiotics that may have an area under the curve above the MIC (AUC/MIC) as the pharmacokinetics/pharmacodynamics (PK/PD) target (*59*).

Resistance studies

We also investigated the propensity for guanidino lipoglycopeptides to select for resistance. When VanA-type VRE was serially passaged over 30 days in sublethal antibiotic concentrations, EVG7 and EVG18 bearing C_7 or chloro-bisphenyl lipids, respectively, resulted in little to no resistance (Fig. 2B). By comparison, greater resistance was selected for against daptomycin, with a 128-fold increase in MIC. These daptomycin-selected isolates did not exhibit cross-resistance to EVG7 (table S10). Similarly, serial MRSA passage

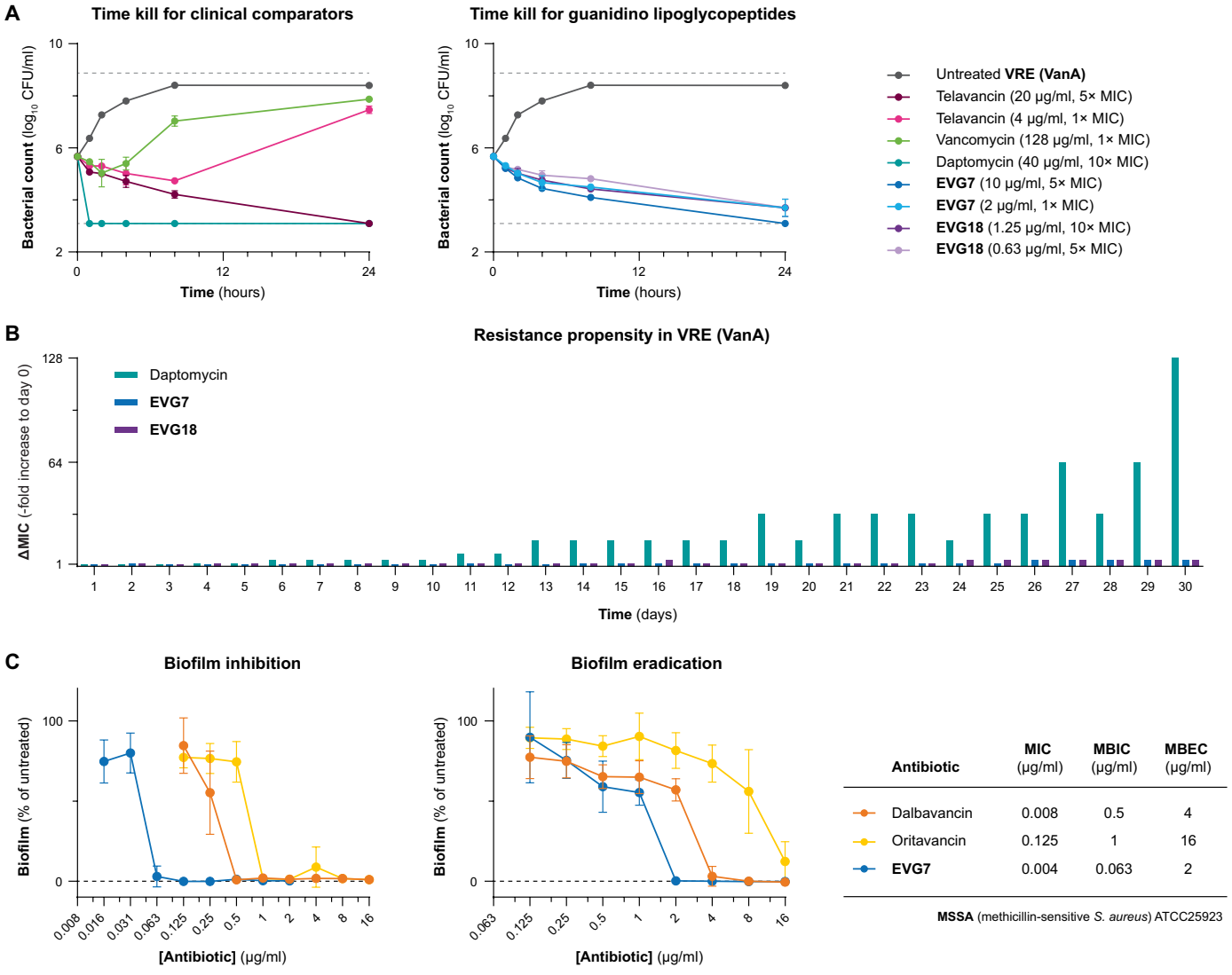

Antibiotic	MIC (μg/ml)	MBIC (μg/ml)	MBEC (μg/ml)
Dalbavancin	0.008	0.5	4
Oritavancin	0.125	1	16
EVG7	0.004	0.063	2

MSSA (methicillin-sensitive *S. aureus*) ATCC25923

Fig. 2. Microbiological characterization. (**A**) Time-kill assay. Bactericidal activity against VanA-type VRE (*E. faecium*) E155 as measured by the $\log_{10}$ CFU per milliliter. Graphical data represent the mean, with error bars showing SD for biological duplicates with technical duplicates. Gray dashed lines represent the limit of detection. (**B**) Resistance selection by serial passage. Change in daily median MIC for VRE (*E. faecium*) E155 compared with day 0 upon continuous exposure to increasing sublethal concentrations of antibiotic. Data are median value (technical triplicate) of a representative biological replicate ($n = 2$). (**C**) Biofilm formation inhibition and eradication of preformed biofilm in MSSA ATCC25923. Data are mean ± SD of biological duplicates with technical quadruplicates. Minimum biofilm inhibitory concentration (MBIC) and minimum biofilm eradication concentration (MBEC) are the median of a minimum of triplicates.

assays revealed minimal resistance for compounds EVG7 and EVG18, whereas resistance to daptomycin rapidly developed (fig. S6). Next, the mutation frequency leading to antibacterial resistance in a VanA-type VRE strain was evaluated (table S11). Resistant mutants were not found for EVG7 at 4× MIC, consistent with a frequency of resistance (FoR) below 6.1×10^{-8}, within the acceptable range for candidate antibacterial agents (*60*). Breakthrough colony formation was observed at lower (2× MIC) dosing of EVG7 after 48 hours, but subculturing showed that these colonies were not authentic resistant mutants. By comparison, an innate FoR of 1.9×10^{-6} was observed for daptomycin at 5× MIC.

Biofilm activity

We next investigated guanidino lipoglycopeptides' anti-biofilm activity. Biofilm formation is a challenge in the treatment of bacterial infections, wherein bacteria form a protective layer capable of blocking antibiotic and immune system activity (*61*). Persistent infections in patients are largely caused by clinical isolates that are strong biofilm producers, with *S. aureus* being one of the main culprits (*62*, *63*). Therefore, we determined the minimal biofilm inhibitory concentration (MBIC) and minimal biofilm eradication concentration (MBEC) against *S. aureus* American Type Culture Collection (ATCC) 25923, a strain reported to form strong biofilms (Fig. 2C) (*64*). EVG7 had an 8- and 16-fold lower MBIC compared with dalbavancin and oritavancin, respectively, and was also a potent biofilm eradicator, with an MBEC of 2 μg/ml, representing a two- and eightfold improved value compared with dalbavancin and oritavancin. Given its potent antibacterial and anti-biofilm activity coupled with its propensity for minimal resistance selection and

low hemolytic activity, EVG7, in which the guanidino moiety is substituted with the linear C_7 lipid, was prioritized for subsequent studies.

Mechanistic studies

Our mechanistic investigations of the guanidino lipoglycopeptides began by examining their capacity to affect the bacterial cell wall. It is well established that vancomycin interferes with late-stage cell wall biosynthesis (*65*), an effect detectable by accumulation of uridine diphosphate (UDP)–MurNAc–pentapeptide (the final soluble precursor in the bacterial cell wall synthesis cycle) upon treatment with cell wall–active antibiotics such as glycopeptides (*65*–*67*). Treatment of *S. aureus* with guanidino lipoglycopeptides also induced UDP-MurNAc-pentapeptide accumulation (Fig. 3A and fig. S7), confirming inhibition of cell wall biosynthesis. Light microscopy was used to image *Bacillus subtilis* in response to antibiotic treatment. Bacterial cells treated with vancomycin, oritavancin, or EVG7 at 5× MIC showed similar cell deformations, with disintegration of the peptidoglycan layer inducing formation of membrane blebs (fig. S8).

We next investigated the impact of guanidino lipoglycopeptides on the cell division regulator MinD in *B. subtilis*. MinD activity is modulated by the membrane potential, and it has been shown that under normal conditions, a green fluorescent protein (GFP)–MinD construct localizes to septum and cell poles. However, once the membrane potential is dissipated, GFP-MinD rapidly delocalizes (*68*). The lipid II–dependent membrane disruptor nisin causes dissipation of the membrane potential, which is visible as a spotty pattern associated with the GFP-MinD construct in the fluorescent microscopy read-out. Contrary to nisin, EVG7 and oritavancin did not induce delocalization of membrane potential–driven GFP-MinD in early exponential phase cultures of *B. subtilis* (Fig. 3B).

Given that lipoglycopeptides exhibit membrane targeting properties (*11*, *69*–*72*), we used membrane-selective fluorescent dyes to determine whether the guanidino lipoglycopeptides also cause membrane disruption. Studies using dipropylthiadicarbocyanine iodide [diSC_3(5)]—a probe that resides on hyperpolarized membranes and is released upon disruption of the membrane potential (*73*)—showed that membrane depolarization was not induced by guanidino lipoglycopeptides (1.5 μg/ml), whereas the known membrane-disrupting and lipid II–targeting antibiotic nisin caused membrane depolarization at the same concentration (fig. S9). In general, EVG7 showed little effect on membrane polarization, even at 16 μg/ml. By comparison, clinically used oritavancin dissipated membrane potential at 16 μg/ml, in keeping with previous reports (*74*, *75*). Membrane perturbation was examined using propidium iodide (PI), a DNA binding dye that can enter cells and fluoresce after pore formation (*76*). In this assay, EVG7 was again found to be less membrane active relative to oritavancin (fig. S10), which is known to induce PI fluorescence in bacterial cells (*75*).

The effect of EVG7 on VRE (strain E155) growth and bacterial cell morphology was examined using scanning electron microscopy (SEM) (Fig. 3C). Treating overnight cultures with EVG7 increased cell clustering, filaments, and lysis. In line with an antibacterial mechanism involving interference with bacterial cell wall biosynthesis, SEM images revealed that EVG7 induced severe membrane damage including perforation-like holes in the cell surface, including ghosts of lysed cells indicative of a bactericidal effect (*77*). By comparison, vancomycin treatment did not cause cell death, as expected for a vancomycin-resistant strain, although it should be noted that there were more nondividing cells in the vancomycin-treated versus the untreated group (fig. S11). Furthermore, we examined the growth and bacterial cell morphology of a vancomycin-sensitive MRSA (strain USA300) (fig. S12), observing a reduction in bacterial cell count along with an increase in cluster size in cultures treated with EVG7 or vancomycin. In both treatment groups, bacterial membranes were affected, resulting in cell lysis. These findings confirm that EVG7 interferes with cell wall biosynthesis in VRE and MRSA, eliciting its bactericidal effect.

Lipid II binding studies

The manner in which vancomycin inhibits cell wall biosynthesis involves sequestration of the cell wall precursor lipid II (*8*–*10*, *78*). A well-defined network of hydrogen bond interactions enables vancomycin to specifically bind to the D-Ala-D-Ala terminus of the lipid II pentapeptide, in turn preventing cell wall cross-linking (*8*–*11*). The binding affinity of vancomycin to lipid II is enhanced by cooperative dimerization (*69*, *79*). Using a lipid II antagonization assay, we confirmed that guanidino lipoglycopeptides retained this lipid II-D-Ala (LII-D-Ala)–dependent mechanism of action. Addition of exogenous LII-D-Ala effectively antagonized the activity of the compounds at 8× MIC, indicating strong lipid II binding (table S12).

We next used isothermal titration calorimetry (ITC; fig. S13) to study lipid II binding to the guanidino lipoglycopeptides. Our initial studies used large unilamellar vesicles (LUVs) composed of 1:3 dioleoylphosphatidylglycerol (DOPG) and dioleoylphosphatidylcholine (DOPC) mimicking the negatively charged bacterial cell surface. When purified LII-D-Ala was included in these LUVs, a strong binding signal was observed for both vancomycin and EVG7, resulting in dissociation constant (K_d) values of 172 and 15 nM, respectively (table S13). EVG7 had a more than 10-fold higher affinity for LII-D-Ala, which is attributable to its lipidated guanidine motif. To further study the effect of this positively charged moiety, we performed binding studies with blank LUVs (not containing lipid II), which showed no interaction with vancomycin but marked binding by EVG7 (see table S13 for full thermodynamic parameters and fig. S14 for all triplicate titrations). To dissect lipid II binding from electrostatic membrane binding effects, we conducted binding studies using neutral LUVs lacking DOPG. Control titrations of blank DOPC LUVs into the sample cell–containing solutions of vancomycin or EVG7 revealed no measurable interaction (fig. S15). When LII-D-Ala–containing vesicles were titrated into the antibiotics, well-defined thermograms were obtained for both vancomycin and EVG7, with K_d values of 1170 and 120 nM, respectively (Fig. 4A and table S14). Although the K_d values obtained using neutral LUVs were higher than those resulting from the use of negatively charged LUVs, the 10-fold tighter binding affinity of EVG7 for LII-D-Ala was maintained.

To further examine how EVG7 maintains potent antibacterial activity against vancomycin-resistant strains, we performed binding studies with a mutated D-Ala-D-Lac form of lipid II (LII-D-Lac), which is known to reduce vancomycin's antibacterial activity (*12*, *13*). ITC studies with neutral LUVs containing LII-D-Lac revealed complete loss of vancomycin binding (Fig. 4B, right). In contrast, titration of neutral LUVs containing LII-D-Lac into a solution of EVG7 produced a marked indication of binding, with a measured K_d value of 813 nM (Fig. 4B, left). Although this indicates a nearly sevenfold reduction in binding affinity relative to wild-type LII-D-Ala, in absolute terms, EVG7 exhibited a higher binding affinity for mutant LII-D-Lac than

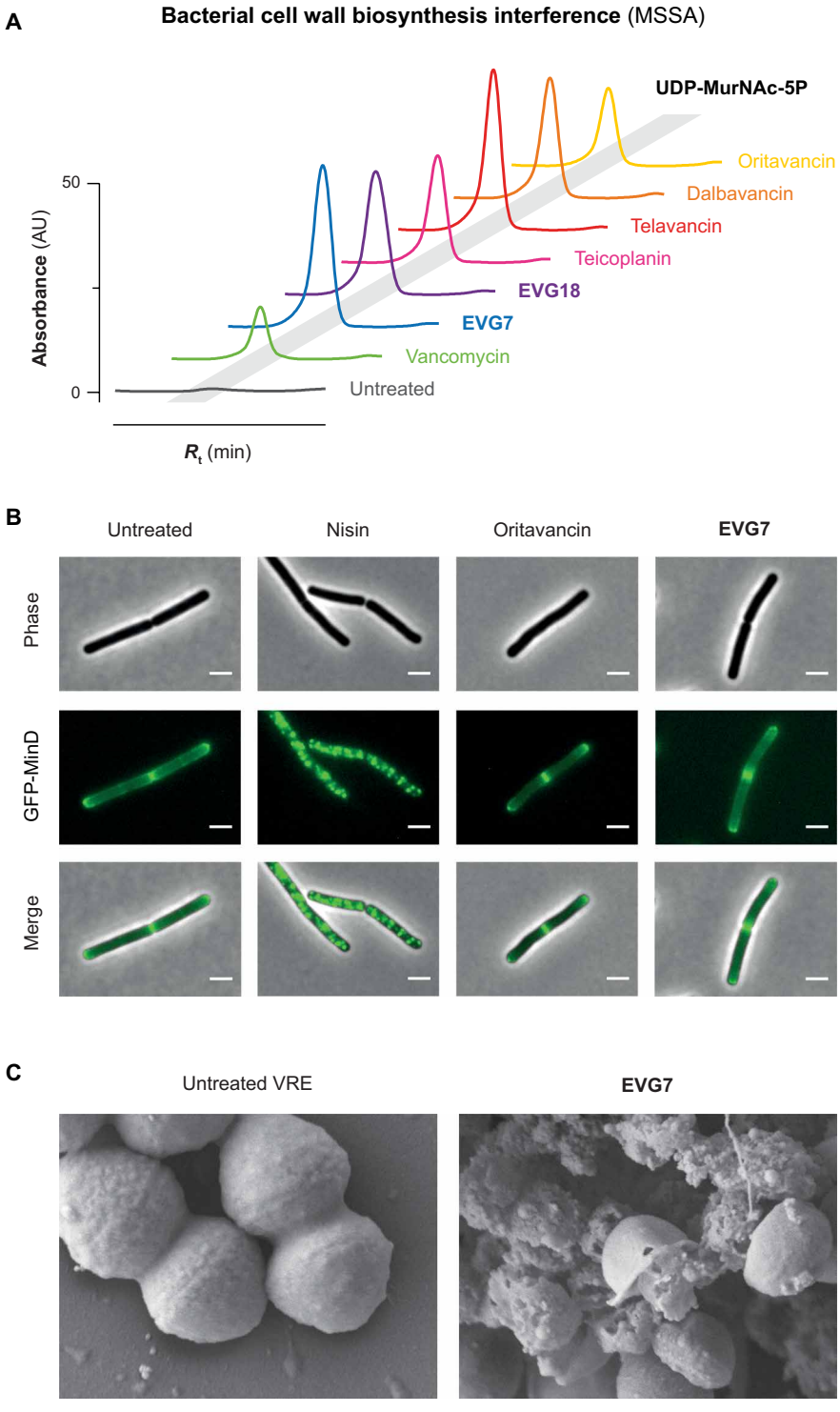

Fig. 3. Interference with bacterial cell wall biosynthesis and membrane integrity. (**A**) UDP-MurNAc-pentapeptide accumulation assay in MSSA ATCC29213. HPLC traces assessing accumulation of UDP-MurNAc-5P upon treatment with (lipo)glycopeptide antibiotic (5 μM) and in untreated control. Full HPLC traces are shown in fig. S7. AU, arbitrary units. (**B**) Microscopic analysis of the membrane potential–dependent localization pattern of GFP-tagged MinD in *B. subtilis* upon treatment (15 min) with membrane-disrupting agent nisin, oritavancin, or EVG7. Scale bars, 2 μm. Images are representative of biological triplicates. (**C**) Structural changes in vancomycin-resistant *E. faecium* E155 upon treatment with EVG7. Scanning electron micrographs of (left) untreated bacterial cultures and (right) cultures treated with EVG7 (at 1× MIC) at ×50,000 magnification. More details in fig. S11.

vancomycin did for native LII-D-Ala (see table S14 for full thermodynamic parameters and fig. S16 for all triplicate titrations).

We next evaluated the capacity for EVG7 to induce cell wall stress responses using bioluminescent reporter strains of *S. aureus* and *B. subtilis* (*80*–*82*). We found that *S. aureus* VraRS-lux and *B. subtilis* LiaI-lux bioreporters were both activated in a dose-dependent manner by EVG7 (fig. S17A). These stress responses are known to be up-regulated by treatment with cell wall–active antibiotics (*80*–*82*). To specifically probe lipid II binding, we examined whether these antibiotic-induced stress responses were antagonized by addition of exogenous LII-D-Ala or LII-D-Lac. Induction of the *B. subtilis* stress response was fully antagonized by LII-D-Ala at a 2:1 lipid II:antibiotic ratio for vancomcyin, EVG7, and oritavancin (Fig. 4C). Furthermore, LII-D-Lac also antagonized the EVG7-induced stress response, albeit at higher concentrations. These findings further substantiate the binding of guanidino lipoglycopeptides to both native D-Ala and mutant D-Lac forms of lipid II as indicated by our ITC studies. Full antagonization by LII-D-Lac is achieved at a 8:1 lipid II:EVG7 ratio (Fig. 4C), similar to oritavancin, which is also known to interact with LII-D-Lac (*83*). By comparison, LII-D-Lac showed little antagonization of the cell wall stress response induced by vancomycin (Fig. 4C), as expected. To confirm the D-Ala-D-Ala motif as the primary target of the guanidino lipoglycopeptides, we performed antagonization studies using wild-type lipid I and the lipid I/II phospholipid carrier undecaprenyl pyrophosphate (C_{55}PP) (fig. S17B). As expected, lipid I effectively antagonized the *B. subtilis* LiaI-lux stress response induced by EVG7, whereas C_{55}PP did not.

We also examined the ability of EVG7 to block various enzymatic processes associated with cell wall synthesis using LII-D-Lac as substrate. Specifically, using TLC-based assays, we studied the capacity for EVG7 to bind and sequester LII-D-Lac leading to inhibition of enzymatic amidation and transglycosylation of lipid II (*84*). EVG7 exhibited a dose-dependent effect on the activities of MurT/GatD (Fig. 4D), which amidates lipid II at the stem peptide Glu residue and penicillin-binding protein 2 (PBP2) (Fig. 4E), which catalyzes lipid II transglycosylation. In general, both enzymatic transformations of LII-D-Lac were fully inhibited at a 10-fold excess of EVG7 . By comparison, PBP2-mediated transglycosylation of wild-type LII-D-Ala was nearly fully inhibited at an equimolar ratio of

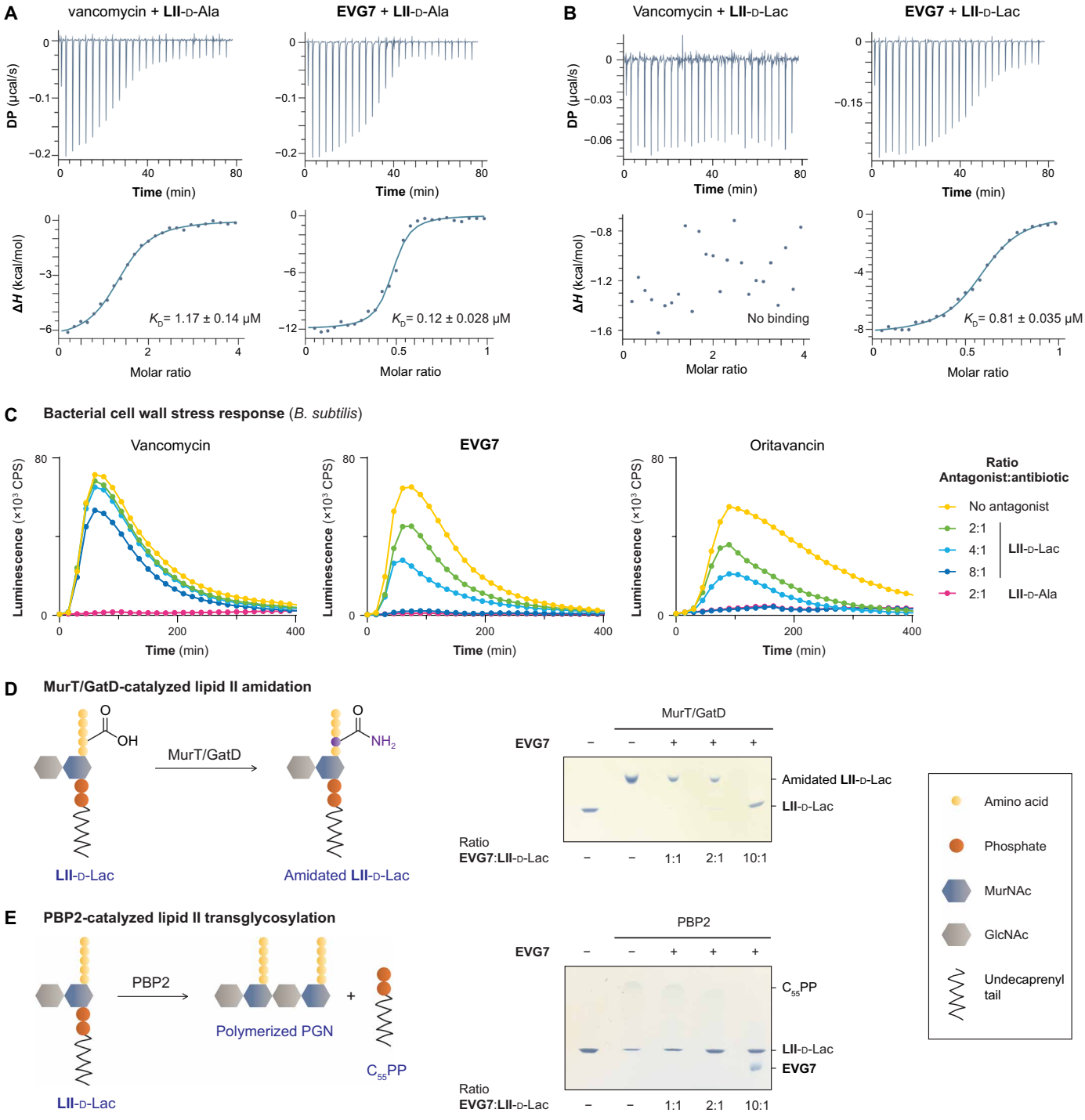

Fig. 4. Mechanism of action studies. (**A**) ITC binding studies. Representative binding thermograms for purified lipid II variant in DOPC LUVs titrated into antibiotic solution. Graphical data are representative for triplicate measurement. Thermodynamic parameters are in table S14. Triplicate titrations are provided in fig. S16. Left: LII-D-Ala (200 µM) in DOPC LUVs (10 mM) titrated into vancomycin (10 µM). Right: LII-D-Ala (100 µM) in DOPC LUVs titrated into EVG7 (20 µM). DP, differential power. (**B**) Left: LII-D-Lac (200 µM) in DOPC LUVs titrated into vancomycin (10 µM). Right: LII-D-Lac (200 µM) in DOPC LUVs titrated into EVG7 (20 µM). (**C**) Antagonism of *Luciferase* cell wall stress response in *B. subtilis* 168 reporter strain TMB1617. Cell wall stress response indicated by luminescence upon treatment with vancomycin, oritavancin, or EVG7, with antagonism by exogenous addition of cell wall precursor (purified LII-D-Ala or LII-D-Lac). Data shown are representative of duplicate. (**D**) Inhibition of MurT/GatD-catalyzed LII-D-Lac amidation. TLC shown is representative of three independent experiments. (**E**) Inhibition of PBP2-catalyzed LII-D-Lac transglycosylation evidenced by reduced formation of C_{55}-PP. TLC shown is representative of three independent experiments.

EVG7, indicating a stronger binding interaction (fig. S18). The capacity for the guanidino lipoglycopeptides to form stable complexes with either wild-type LII-D-Ala or mutant LII-D-Lac was also assessed using a TLC-based assay. This indicated that EVG7, vancomycin, and oritavancin all formed extraction-stable complexes with LII-D-Ala at a 2:1 molar ratio (glycopeptide:LII) (fig. S19), indicating potential dimerization, which is not uncommon for glycopeptide antibiotics (*69*, *79*). In contrast, EVG7 did not form an extraction-stable complex with LII-D-Lac, nor did vancomycin or oritavancin.

In vivo efficacy studies

The performance of EVG7 in the above mechanistic and in vitro cell–based assays led to its further evaluation in in vivo models. Initial tolerability studies in mice revealed that EVG7 was well tolerated at doses up to 100 mg/kg administered subcutaneously (SC) and 30 mg/kg administered intravenously (iv) (table S15). When dosed at 3 mg/kg sc or iv, PK analysis indicated that EVG7 has a clearance half-life of 1.2 and 0.90 hours, respectively (Table 2, fig. S20, and table S16). Blood concentrations of EVG7 were maintained above MIC (against MRSA USA300) for >8 hours for subcutaneous dosing and >4 hours for intravenous dosing, indicating good exposure (fig. S20).

Subsequently, in vivo efficacy was assessed using an established MRSA murine thigh infection model (*85*). Immunosuppressed mice were infected with MRSA and subsequently treated with vehicle, EVG7 (3, 10, 30, or 100 mg/kg SC, q6h), or vancomycin (25 mg/kg, iv, q12h) as a clinical comparator antibiotic (Fig. 5A). The lowest dose evaluated for EVG7 (3 mg/kg, SC, q6h, total cumulative dose of 12 mg/kg) resulted in a near 6-log reduction in bacterial titer compared with vehicle treatment. This response compares well with that seen in the vancomycin group, which was treated with a much higher dose (25 mg/kg, iv, q12h, total cumulative dose of 50 mg/kg). Furthermore, when EVG7 dosing was increased to 10, 30, or 100 mg/kg (sc, q6h, total cumulative dose of 40, 120, or 400 mg/kg), an even greater reduction in bacterial load was achieved. Overall, EVG7 displayed a dose-dependent effect and was bactericidal at all tested doses, reducing bacterial burden significantly ($P \leq 0.0001$) (Fig. 5A and tables S17 and S18). Given these findings, we next evaluated intravenous efficacy with the same dosing frequency as the vancomycin comparator (Fig. 5B). In this case, a pronounced and similar effect was observed at all doses tested (3, 10, and 25 mg/kg, iv, q12h). The lowest EVG7 treatment group (3 mg/kg) resulted in a 6-log reduction of bacterial thigh burden compared with vehicle control and a significant ($P < 0.0001$) reduction compared with vancomycin control (Fig. 5B and tables S19 and S20). These findings mirror the result of the MIC assays (Table 1), demonstrating that EVG7 activity is superior to vancomycin both in vitro and in vivo.

The capacity for guanidino lipoglycopeptides to treat systemic infection in vivo was next investigated in a 7-day sepsis survival study using immunocompetent mice intravenously infected with *S. aureus* NCTC8178. One hour postinfection, treatment over a 24-hour period commenced with EVG7 dosed at different regimens, vancomycin (25 mg/kg, iv, q12h), or vehicle, after which survival was monitored for a total of 169 hours (Fig. 5C). Mice receiving vehicle only survived 51.3 hours on average, whereas vancomycin-treated mice had a mean survival of 131.5 hours, with only 1 of 10 mice surviving to the end of day 7. In contrast, in the EVG7-treated group dosed according to the same regimen as the vancomycin group (25 mg/kg, iv, q12h, total cumulative dose of 50 mg/kg), all mice survived to the end of the study (≥169 hours survival). When administered at lower doses, EVG7 still outperformed vancomycin. In the groups treated with EVG7 at 10 mg/kg (sc, q6h, total cumulative dose of 40 mg/kg) or 3 mg/kg (sc, q6h, total cumulative dose of 12 mg/kg), 10 of 10 mice and 9 of 10 mice, respectively, survived to the 7-day endpoint (tables S21 to S23). Building on these findings, we also examined the organ-specific effect of EVG7 in reducing *S. aureus* NCTC8178 bacterial burden. This involved a sepsis model wherein immunocompetent mice were intravenously infected with *S. aureus*, after which they were treated with either vehicle or antibiotic for 24 hours and monitored for an additional 25 hours. The animals were then euthanized, and the bacterial burden in the spleen, kidneys, and heart was assessed (Fig. 5D). The bacterial burden in the spleens of the mice that received no antibiotic was reduced by approximately 3-log compared with pretreatment, an effect ascribed to the immune systems of the mice. Vancomycin (25 mg/kg, iv, q12h) did not reduce the spleen burden relative to the vehicle treated group, whereas EVG7 administered at the same dose and frequency reduced bacterial burden approximately 1-log fold (Fig. 5D and tables S24 and S25). In the kidneys, the bacterial burden in the vehicle-treated group increased, whereas an antibiotic effect was observed for both vancomycin and EVG7. Vancomycin treatment (25 mg/kg, iv, q12h) resulted in a near 4-log decrease in bacterial burden relative to vehicle. By comparison, the same dosing of EVG7 more effectively reduced the kidney burden, resulting in an almost 6-log decrease compared with vehicle. Furthermore, a lower total dose of EVG7 (10 mg/kg, sc, q6h) outperformed vancomycin, reducing the kidney burden >1-log fold more (Fig. 5D and tables S24 and S26). In the heart, vancomycin (25 mg/kg, iv, q12h) and EVG7 (dosed at either 25 mg/kg, iv, q12h, or 10 mg/kg, SC, q6h) caused similar reductions in bacterial burden (~3-log fold compared with vehicle) (Fig. 5D and tables S24 and S27).

In vitro toxicity and pharmacology

EVG7 was further evaluated in cytotoxicity screens using HepG2 and human embryonic kidney (HEK) 293 cells (Table 2). EVG7 was not cytotoxic up to the highest concentration tested (100 μM), even when using only 1% fetal bovine serum (FBS) to ensure low plasma protein binding and therefore high compound availability (*86*). EVG7 was found to be notably less toxic in these cell-based assays than the clinically used lipoglycopeptides telavancin and oritavancin (fig. S21).

The mutagenic potential of EVG7 was assessed in an Ames reverse mutation assay in the absence and presence of S9 metabolic activation (Table 2 and table S28). EVG7 exhibited no mutagenic potential in *Salmonella typhimurium* TA98 (detection of frameshift mutations) and TA100 (detection of base-pair substitutions), up to the highest concentration tested (1.1 mM, 2 mg/ml). Next, genotoxicity was evaluated in an in vitro micronucleus test in the human lymphoblast cell line TK6. In this assay, treatment with genotoxic agents results in the formation of micronuclei within daughter cells after cell division, an effect that was not observed for EVG7 at any of the concentrations tested (Table 2 and tables S29 and S30).

Secondary pharmacology of EVG7 was further evaluated against a commercial panel of common antitargets (*87*), resulting in identification of five hits upon treatment with EVG7 at 10 μM (Table 2, table S31, and fig. S22). Four of the five hits are predominantly

Table 2. ADMET properties for guanidino lipoglycopeptide antibiotic EVG7. CC_{50}, half-maximal cytotoxicity concentration; KOP, kappa opioid receptor; NET, norephinedrine transporter; CYP, cytochrome P450; *t*½, half-life; CL_{int}, intrinsic clearance rate; C_{max}, maximum serum concentration; CL, clearance rate.

Experiment	Parameter	EVG7			
Cytotoxicity	CC_{50} (μM)				
HepG2		>100			
HEK293		>100			
Ames mutagenicity	Result at 2 mg/ml				
TA098 (−S9/+S9)	Frameshift mutations	(–)/(–)			
TA100 (−S9/+S9)	Base-pair substitutions	(–)/(–)			
Micronucleus genotoxicity	Result at 120 μg/ml				
TK6 (−S9/+S9)		(–)/(–)			
Antitarget binding	IC_{50} (μM)				
D_{2s}		5.1 ± 1.0			
KOP		6.1 ± 0.65			
5-HT2B		8.5 ± 1.6			
NET		10 ± 0.89			
Cardiac ion channel inhibition	IC_{50} (μM)				
hERG		16 ± 0.89			
hKv7.1		94 ± 16			
hKv4.3		59 ± 2.9			
hKir2.1		>100			
hNav1.5 (peak)		40 ± 5.3			
hNav1.5 (late)		62 ± 5.4			
hCav1.2		53 ± 4.5			
CYP450 inhibition in HLM	IC_{50} (μM)				
CYP1A2		>100			
CYP2B6		142 ± 205			
CYP2C8		55 ± 44			
CYP2C9		>100			
CYP2C19		>100			
CYP2D6		4.3 ± 0.25			
CYP3A4 (midazolam as substrate)		67 ± 24			
CYP3A4 (testosterone as substrate)		>100			
		Mouse	*Rat*	*Dog*	*Human*
Plasma stability	*t*½ (min)	>120	>120	>120	>120
Microsomal stability	*t*½ (min)	92 ± 28	89 ± 22	97 ± 22	405 ± 252
	CL_{int} (μl/min/mg)	75 ± 23	78 ± 19	72 ± 17	17 ± 11
Plasma protein binding	(% bound)	91 ± 3.3	94 ± 1.4	67 ± 3.6	94 ± 3.3
		SC		*IV*	
Tolerability					
Mouse	Tolerated dose (mg/kg)	100		30	
Pharmacokinetics					
Mouse (3 mg/kg)	*t*½ (hours)	1.22 ± 0.196		0.896 ± 0.234	
	C_{max} (μM)	1.07 ± 0.139		3.15 ± 0.614	
	AUC_{0-last} (hour*μg/ml)	5.31 ± 0.507		4.14 ± 0.514	
	CL (ml/min/kg)	9.30 ± 0.944		12.1 ± 1.52	

(Continued)

(Continued)

Experiment	Parameter	EVG7
Rat (3 mg/kg)	$t½$ (hours)	1.11 ± 0.02
	C_{max} (μM)	7.75 ± 0.493
	AUC_{0-last} (hour*μg/ml)	7.17 ± 0.197
	CL (ml/min/kg)	6.93 ± 0.2

found in the central nervous system and therefore unlikely to have clinical implications given that glycopeptide antibiotics are generally not blood-brain barrier permeable and have poor penetration into the cerebrospinal fluid (*88*). The fifth hit was the cardiac potassium channel hERG, a well-established antitarget that is also commonly identified as a target of second-generation lipoglycopeptide antibiotics (*89*, *90*). A similar in vitro effect on hERG was previously reported in the preclinical assessment of oritavancin [half-maximal inhibitory concentration (IC_{50}) = 22 μM] (*91*) that was subsequently found to pose no serious clinical cardiotoxicity risk (*90*, *91*). Further assessment of EVG7 against a panel of human cardiac ion channels revealed the hERG effect to be most prominent, with an IC_{50} of 16 μM (28 μg/ml), with comparatively lower effects on the other cardiac ion channels tested (Table 2 and fig. S23). Last, the impact of EVG7 on cytochrome P450-mediated metabolism was examined by monitoring isoform-specific metabolites in human liver microsomes (HLMs). EVG7 showed low to no inhibition of most hepatic CYP450 isoenzymes (Table 2 and fig. S24) and mild inhibition of CYP2D6 in a concentration-dependent manner, with an IC_{50} of 4 μM (7 μg/ml).

EVG7 in vitro plasma stability, microsomal stability, and plasma protein binding were next assessed in plasma and liver microsomes of mouse, rat, dog, and human origin. EVG7 showed high plasma stability, with half-lives exceeding 3 hours in all species (Table 2 and fig. S25). In vitro assessment of microsomal clearance revealed a species-dependent effect (Table 2 and fig. S26). In the presence of HLMs, EVG7 showed high stability, with a $t½$ greater than 6 hours, whereas for mouse, rat, and dog liver microsomes, the $t½$ was ~1.5 hours. EVG7 was found to exhibit high plasma protein binding in plasma from all species tested (Table 2 and fig. S27), in line with reported protein binding for lipoglycopeptide antibiotics (*34*, *92*).

In vivo toxicity

Last, the toxicity of EVG7 was investigated in rats in comparison with vancomycin. Study doses and route of administration were designed after confirmation of exposures in a rat PK study (Table 2, fig. S28, and table S32). This showed a plasma half-life of 1.11 hours for EVG7 (3 mg/kg, single intravenous dosing), similar to the 1.6-hour half-life reported for vancomycin (10 mg/kg, single intravenous dosing) (*34*). EVG7 was evaluated for toxicity in a 7-day repeat dose study in comparison with vancomycin in rats with twice daily intravenous bolus injection. Both compounds were tested at two doses: EVG7 was administered at 3 mg/kg per dose (6 mg/kg per day) and 15 mg/kg per dose (30 mg/kg per day), with vancomycin dosed at 40 mg/kg per dose (80 mg/kg per day) and 200 mg/kg per dose (400 mg/kg per day). The low dose for EVG7 corresponded to the lowest effective dose in the murine thigh infection model. The higher vancomycin dose was selected on the basis of previous reported experience of kidney effects induced by vancomycin in renal toxicity studies (*93*). In a 7-day repeat dose study in rats, EVG7 up to 30 mg/kg per day had no effect on body weight, was well tolerated (table S33), and showed no kidney adverse effects, with minimal to mild tubular necrosis (fig. S29 and tables S34 and S35). In contrast, vancomycin at 400 mg/kg per day induced changes in serum biomarkers of renal function (creatinine and urea) at day 8 (fig. S30), accompanied by severe acute tubular necrosis (fig. S29 and table S35).

DISCUSSION

In recent years, semisynthetic lipoglycopeptides such as clinically approved telavancin, dalbavancin, and oritavancin have proven important additions to this arsenal, particularly in light of growing vancomycin resistance (*11*, *94*). We here report a class of highly active semisynthetic lipoglycopeptides containing a basic guanidino group bearing a lipid tail. In most cases, guanidino lipoglycopeptide MIC values were much lower than for vancomycin, typically translating to 100- or 1000-fold increases in activity. Serum addition had little impact on the activity of most guanidino lipoglycopeptides, predictive of good availability in vivo (*54*–*56*, *95*–*98*). EVG7 does not display nonspecific membrane activity, as evidenced by its low propensity to cause membrane permeabilization or depolarization. The absence of such effects is typically seen as favorable, given that antibacterial agents that function via membrane disruption are often linked to perturbation of mammalian cell membranes, leading to off-target effects and toxicity (*71, 99*).

Guanidino lipoglycopeptides display enhanced antibacterial activity, but this is not due to accelerated killing kinetics as indicated by their similarity with the time-kill curves obtained with glycopeptides vancomycin (*100, 101*), teicoplanin (*100*), telavancin (*101*), and dalbavancin (*101*). Pharmacodynamic characterization in vitro of EVG7 indicated that the slope for the concentration-effect relationship of EVG7 is substantially steeper than that of vancomycin. Also, given that AUC/MIC is the PK/PD target for all clinically used glycopeptide antibiotics (*102*–*104*), it is expected that the same will be true for EVG7. The future determination of the specific fAUC/MIC target exposure for EVG7 will serve to guide dose selection in clinical studies.

Mechanistically, the guanidino lipoglycopeptides maintain the lipid II–dependent mechanism of action common to all glycopeptides causing inhibition of late-stage cell wall biosynthesis. Of note

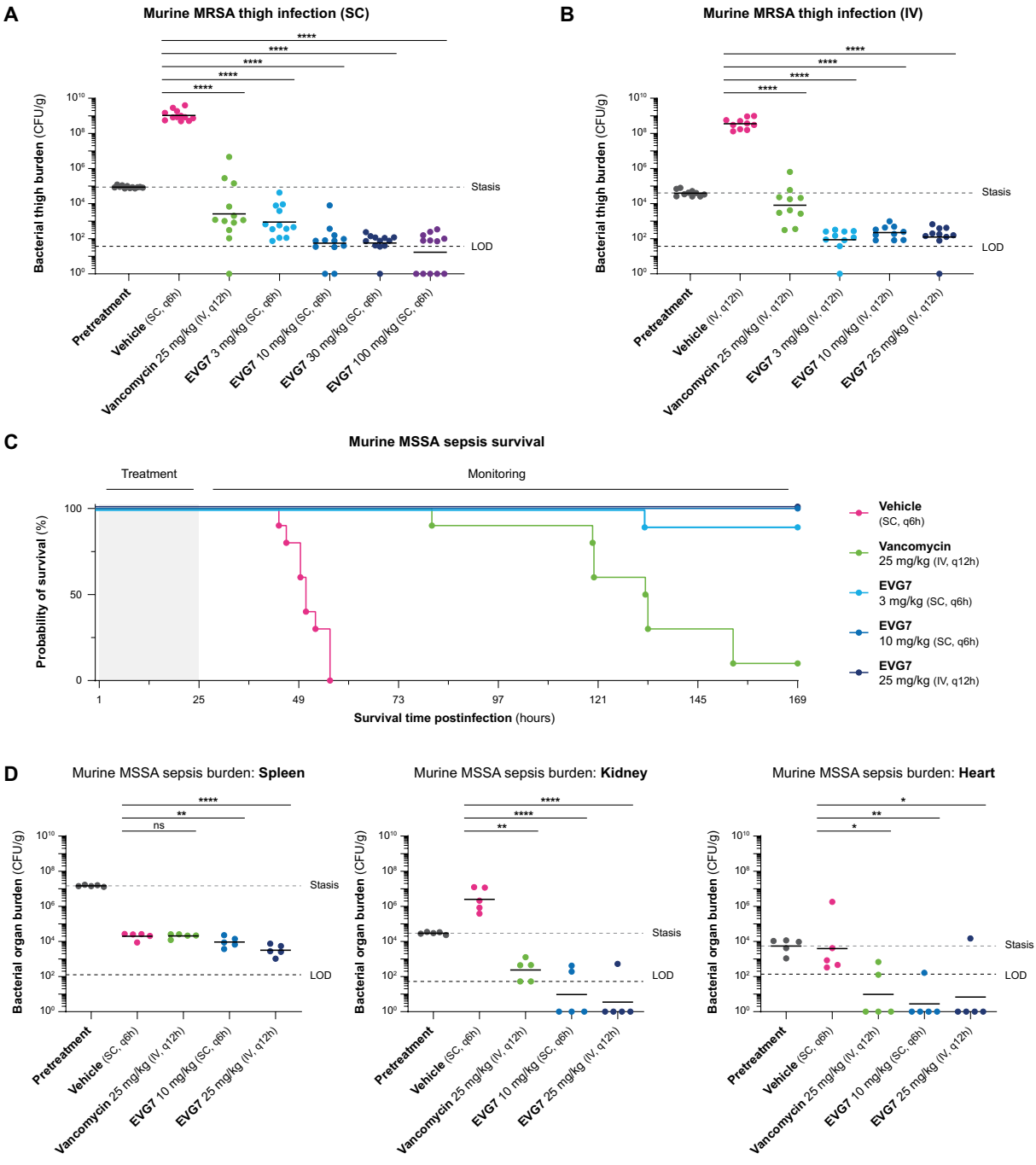

Fig. 5. In vivo efficacy studies. Samples with bacterial burden below limit of detection (LOD) were assigned a value of 1 colony-forming unit per gram homogenized tissue (CFU/g) for graphical and statistical purposes. Groups were compared by Kruskal-Wallis test using the Conover-Inman test (to make all pairwise comparisons between groups). (**A**) Murine thigh infection model with EVG7 subcutaneous administration. One hour postinfection with MRSA strain NRS384 (USA300-0114), immunocompromised mice were treated with antibiotic at concentration and dosing indicated ($n = 6$ per group) and euthanized 23 hours postinfection. Data show bacterial burden in each individual thigh, with a line at the geometric mean ($n = 12$; two thighs per mouse). Details and statistical analysis are in tables S17 and S18. (**B**) Murine thigh infection model with intravenous administration of EVG7. One hour postinfection with MRSA strain NRS384 (USA300-0114), immunocompromised mice were treated with antibiotic ($n = 5$ per group) and euthanized 21.5 hours postinfection. Graphical data show bacterial burden in each individual thigh, with a line at the geometric mean ($n = 10$; two thighs per mouse). Details and statistical analysis are in tables S19 and S20. (**C**) Murine sepsis survival study. Kaplan-Meier plot for survival of immunocompetent CD1 mice infected with MSSA NCTC8178. One hour postinfection, mice were treated with antibiotic for 24 hours ($n = 10$ per group), and survival was monitored for 7 days. Details and statistical analysis are in tables S21 to S23. (**D**) Murine sepsis burden study. Bacterial burden in spleen (left), kidney (middle), and heart (right) tissue of immunocompetent CD1 mice after infection with MSSA NCTC8178, treatment with antibiotic for 24 hours, and euthanasia 49 hours postinfection. Graphical data show bacterial burden for each mouse, with a line at the geometric mean ($n = 5$). Details and statistical analysis are in tables S24 to S27. *$P = 0.1$ to 0.01, **$P = 0.01$ to 0.001, and ****$P \leq 0.0001$. ns, not significant.

is that in LUVs mimicking the bacterial membrane, the binding affinity of EVG7 for LII-D-Ala was nearly 10 times greater than that of vancomycin and EVG7 also maintained strong binding to mutant lipid II (LII-D-Lac), which is commonly associated with vancomycin resistance, providing an explanation for its increased antibacterial activity. These findings suggest that the lipidated guanidino motif of EVG7 provides a combination of productive electrostatic interactions and membrane anchoring with the negatively charged bacterial cell surface, thereby compensating for the reduced binding affinity associated with the D-Ala to D-Lac mutation.

Guanidino lipoglycopeptides also showed enhanced aqueous solubility relative to clinically used lipoglycopeptides, an effect attributable to their highly basic guanidine motif; at physiological pH, the guanidine moiety is fully protonated, thus providing a highly delocalized positive charge that promotes increased aqueous solubility. EVG7 was found to have excellent stability in both plasma and liver microsomes along with high plasma protein binding, as is typical for lipoglycopeptides (*92*). Pharmacological evaluation of EVG7 showed low-to-no affinity for common antitargets and CYP enzymes. The observed blockage of hERG by EVG7 was anticipated given previous reports of similar effects among clinically approved lipoglycopeptide antibiotics (*89*, *90*). The IC_{50} of EVG7 for hERG was more than 30-fold higher than the C_{max} (free) for single dosing mice at 3 mg/kg iv or sc, providing a therapeutic window that is expected to avoid clinical cardiotoxicity (*105*). The enhanced antibacterial activity observed for guanidino lipoglycopeptides may allow for lower dosing, which, along with their favorable toxicity profile, suggests that they may provide an alternative to current clinically used glycopeptides. Investigation of the organ-specific effects of EVG7 also shows it to be superior to vancomycin in reducing the infection burden in the spleen, kidney, and heart. The effectiveness of EVG7 in clearing *S. aureus* infection in the heart indicates that guanidino lipoglycopeptides may potentially be useful in treating infective endocarditis (IE)—a condition commonly related to *S. aureus* biofilm formation (*63*) that EVG7 was able to successfully inhibit/eradicate in vitro. Clinically, the treatment of IE presents a major challenge, with a 20% morbidity rate in the first 30 days of disease (*106*). Although glycopeptide therapy with dalbavancin has recently been reported as a promising treatment option for IE (*107*, *108*), nonsusceptible strains and glycopeptide-induced IE have also been reported (*109*, *110*), underscoring the need for additional effective treatments.

Clinical use of vancomycin is complicated by the potential to cause acute kidney injury at therapeutically relevant doses, especially in critically ill patients with serious infections, restricting both dose and concomitant use of other nephrotoxic agents (*111*). We found minimal to mild kidney effects in rats in a repeat dose study for EVG7 at the supratherapeutic dose of 30 mg/kg per day in comparison with a dose of vancomycin at 400 mg/kg per day, where (severe) acute tubule injury was apparent, which may indicate an improved therapeutic safety profile of EVG7.

There are limitations in our study worthy of mention. Despite showing efficacy against various Gram-positive pathogens, the in vivo efficacy data presented are limited to two murine infection models. Furthermore, the in vivo nephrotoxicity data presented are based on a single 7-day repeat dose study in rats. EVG7 is likely subject to renal clearance, and future studies should therefore pay specific attention to its potential to cause kidney effects at high doses. In addition, to enable preclinical estimates for the efficacious dosing of EVG7 in humans, key parameters such as the PK/PD driver, biodistribution, and tissue penetration will need to be established in (larger) animal models. Last, the clinical potential of EVG7 cannot be fully realized until safety and efficacy are demonstrated in human clinical trials.

In summary, we report the development of the guanidino lipoglycopeptides, a promising class of semisynthetic glycopeptide antibiotics. These compounds, specifically EVG7, showed potent antibacterial activity and promising toxicity profiles. Further assessment using advanced in vivo models will be the next step toward a more complete characterization of their toxicity and PK/PD profiles as well as establishment of their clinical potential for the treatment of serious Gram-positive infections.

MATERIALS AND METHODS

Study design

The objective of this work was to evaluate the in vitro and in vivo efficacy and safety of the guanidino lipoglycopeptides. The in vivo studies were designed to investigate antibacterial efficacy (*S. aureus* murine thigh infection and murine sepsis survival/burden), PK profile (PK in mice and rats), and (nephro)toxicity (7-day repeat dose study in rats). Sample sizes were determined on the basis of prior studies to achieve statistical significance. No animals were excluded from analysis. No documented method of randomization was used, with animals randomly assigned to groups on arrival in the animal facility. All animal procedures at Evotec Ltd. (UK) were performed under UK Home Office Licence PA67E0BAA, with local ethical committee clearance. Colony counting and data analysis were performed with the operator blinded to the treatment of each animal. Animal procedures at Pharmacology Discovery Services Taiwan Ltd. (Taiwan) were performed in general accordance with the "Guide for the Care and Use of Laboratory Animals: Eighth Edition" (*112*) under Office of Laboratory Animal Welfare (OLAW) assurance F16-00213 (A5890-01), with local ethical committee (Institutional Animal Care and Use Committee) clearance. Animal procedures at Pharmaron, Beijing (China) were performed under non-GLP conditions with local ethical committee clearance, Animal Use Protocol number: IVP-Tox-04232024. Additional materials and methods can be found in the Supplementary Materials.

Bacterial strains

All ATCC reference strains were commercially obtained or provided by Leiden University Medical Center (LUMC, Leiden, the Netherlands). MRSA USA300 is a clinical isolate from the Texas Children's Hospital. The *E. faecium* and *E. faecalis* strains were provided by the laboratory for medical microbiology at the University Medical Center Utrecht (Utrecht, the Netherlands). The *S. aureus* clinical isolates in the extended panel of MRSA and BORSA strains were retrieved from the collection of the clinical microbiology laboratory at the LUMC (Leiden, the Netherlands). The other *S. aureus* clinical isolates (MRSA, VISA, and VRSA) were supplied by the Network on Antimicrobial Resistance in *S. aureus* (NARSA) via Biodefense and Emerging Infections Research Resources Repository, National Institute of Allergy and Infectious Diseases (NIAID), National Institutes of Health (NIH).

Statistical analysis

Data plotting and fitting were performed in GraphPad Prism v9.0.0. For the murine efficacy studies, data analysis from the culture

burdens was performed with StatsDirect software v3.2.8 using appropriate nonparametric statistical models (Kruskal-Wallis using Conover-Inman to make all pairwise comparisons between groups) and compared with vehicle-treated animals. For the PK study in rats, PK parameters were reported from noncompartmental analysis of the plasma data using WinNonlin (best-fit mode). For the 7-day repeat dose study in rats, group comparisons were performed in GraphPad Prism v10.1.2 using nonparametric (unpaired) Mann-Whitney tests, with two-tailed P values < 0.05 considered statistically significant, without further correction.

Supplementary Materials

This PDF file includes:
Materials and Methods
Figs. S1 to S30
Tables S1 to S35
References (*113*–*142*)

Other Supplementary Material for this manuscript includes the following:
Data file S1
MDAR Reproducibility Checklist

REFERENCES AND NOTES

1. World Health Organization, "Antimicrobial resistance global report on surveillance (2014)"; https://iris.who.int/handle/10665/112642.
2. Centers for Disease Control and Prevention (U.S.), *Antibiotic Resistance Threats in the United States, 2019* (2019); http://dx.doi.org/10.15620/cdc:82532.
3. S. J. Van Hal, V. G. Fowler, Is it time to replace vancomycin in the treatment of methicillin-resistant *Staphylococcus aureus* infections? *Clin. Infect. Dis.* **56**, 1779–1788 (2013).
4. W. A. McGuinness, N. Malachowa, F. R. Deleo, Vancomycin resistance in *Staphylococcus aureus*. *Yale J. Biol. Med.* **90**, 269–281 (2017).
5. S. Adani, T. Bhowmick, M. P. Weinstein, N. Narayanan, Impact of vancomycin MIC on clinical outcomes of patients with methicillin-resistant *Staphylococcus aureus* bacteremia treated with vancomycin at an institution with suppressed MIC reporting. *Antimicrob. Agents Chemother.* **62**, e02512–e02517 (2018).
6. A. Cassini, L. D. Högberg, D. Plachouras, A. Quattrocchi, A. Hoxha, G. S. Simonsen, M. Colomb-Cotinat, M. E. Kretzschmar, B. Devleesschauwer, M. Cecchini, D. A. Ouakrim, T. C. Oliveira, M. J. Struelens, C. Suetens, D. L. Monnet; Burden of AMR Collaborative Group, Attributable deaths and disability-adjusted life-years caused by infections with antibiotic-resistant bacteria in the EU and the European Economic Area in 2015: A population-level modelling analysis. *Lancet Infect. Dis.* **19**, 56–66 (2019).
7. Antimicrobial Resistance Collaborators, Global burden of bacterial antimicrobial resistance in 2019: A systematic analysis. *Lancet* **399**, 629–655 (2022).
8. J. Pootoolal, J. Neu, G. D. Wright, Glycopeptide antibiotic resistance. *Annu. Rev. Pharmacol. Toxicol.* **42**, 381–408 (2002).
9. C. T. Walsh, S. L. Fisher, I. S. Park, M. Prahalad, Z. Wu, Bacterial resistance to vancomycin: Five genes and one missing hydrogen bond tell the story. *Chem. Biol.* **3**, 21–28 (1996).
10. J. C. Barna, D. H. Williams, The structure and mode of action of glycopeptide antibiotics of the vancomycin group. *Annu. Rev. Microbiol.* **38**, 339–357 (1984).
11. M. A. T. Blaskovich, K. A. Hansford, M. S. Butler, Z. Jia, A. E. Mark, M. A. Cooper, Developments in glycopeptide antibiotics. *ACS Infect Dis* **4**, 715–735 (2018).
12. C. C. McComas, B. M. Crowley, D. L. Boger, Partitioning the loss in vancomycin binding affinity for D-Ala-D-Lac into lost H-bond and repulsive lone pair contributions. *J. Am. Chem. Soc.* **125**, 9314–9315 (2003).
13. T. D. H. Bugg, G. D. Wright, S. Dutka-Malen, M. Arthur, P. Courvalin, C. T. Walsh, Molecular basis for vancomycin resistance in *Enterococcus faecium* BM4147: Biosynthesis of a depsipeptide peptidoglycan precursor by vancomycin resistance proteins VanH and VanA. *Biochemistry* **30**, 10408–10415 (1991).
14. M. Arthur, R. J. Quintiliani, Regulation of VanA- and VanB-type glycopeptide resistance in enterococci. *Antimicrob. Agents Chemother.* **45**, 375–381 (2001).
15. P. Courvalin, Resistance of enterococci to glycopeptides. *Antimicrob. Agents Chemother.* **34**, 2291–2296 (1990).
16. L. Cui, X. Ma, K. Sato, K. Okuma, F. C. Tenover, E. M. Mamizuka, C. G. Gemmell, M.-N. Kim, M.-C. Ploy, N. E. Solh, V. Ferraz, K. Hiramatsu, Cell wall thickening is a common feature of vancomycin resistance in *Staphylococcus aureus*. *J. Clin. Microbiol.* **41**, 5–14 (2003).
17. B. P. Howden, J. K. Davies, P. D. R. Johnson, T. P. Stinear, M. L. Grayson, Reduced vancomycin susceptibility in *Staphylococcus aureus*, including vancomycin-intermediate and heterogeneous vancomycin-intermediate strains: Resistance mechanisms, laboratory detection, and clinical implications. *Clin. Microbiol. Rev.* **23**, 99–139 (2010).
18. M. K. Hayden, K. Rezai, R. A. Hayes, K. Lolans, J. P. Quinn, R. A. Weinstein, Development of daptomycin resistance in vivo in methicillin-resistant *Staphylococcus aureus*. *J. Clin. Microbiol.* **43**, 5285–5287 (2005).
19. T. T. Tran, J. M. Munita, C. A. Arias, Mechanisms of drug resistance: Daptomycin resistance. *Ann. N. Y. Acad. Sci.* **1354**, 32–53 (2015).
20. B. Gu, T. Kelesidis, S. Tsiodras, J. Hindler, R. M. Humphries, The emerging problem of linezolid-resistant *Staphylococcus*. *J. Antimicrob. Chemother.* **68**, 4–11 (2013).
21. R. D. Gonzales, P. C. Schreckenberger, M. Beth Graham, S. Kelkar, K. DenBesten, J. P. Quinn, Infections due to vancomycin-resistant *Enterococcus faecium* resistant to linezolid. *Lancet* **357**, 1179 (2001).
22. S. L. Barriere, The ATTAIN trials: Efficacy and safety of telavancin compared with vancomycin for the treatment of hospital-acquired and ventilator-associated bacterial pneumonia. *Future Microbiol.* **9**, 281–289 (2014).
23. G. G. Zhanel, D. Calic, F. Schweizer, S. Zelenitsky, H. Adam, P. R. S. Lagacé-Wiens, E. Rubinstein, A. S. Gin, D. J. Hoban, J. A. Karlowsky, New lipoglycopeptides: A comparative review of dalbavancin, oritavancin and telavancin. *Drugs* **70**, 859–886 (2010).
24. J. A. Karlowsky, K. Nichol, G. G. Zhanel, Telavancin: Mechanisms of action, in vitro activity, and mechanisms of resistance. *Clin. Infect. Dis.* **61**, S58–S68 (2015).
25. D. J. Cada, D. E. Baker, Oritavancin diphosphate. *Hosp. Pharm.* **49**, 1049–1063 (2014).
26. E. van Groesen, P. Innocenti, N. I. Martin, Recent advances in the development of semisynthetic glycopeptide antibiotics: 2014–2022. *ACS Infect. Dis.* **8**, 1381–1407 (2022).
27. E. van Groesen, C. J. Slingerland, P. Innocenti, M. Mihajlovic, R. Masereeuw, N. I. Martin, Vancomyxins: Vancomycin-polymyxin nonapeptide conjugates that retain anti-Gram-positive activity with enhanced potency against Gram-negative strains. *ACS Infect. Dis.* **7**, 2746–2754 (2021).
28. W. Shi, F. Chen, X. Zou, S. Jiao, S. Wang, Y. Hu, L. Lan, F. Tang, W. Huang, Design, synthesis, and antibacterial evaluation of vancomycin-LPS binding peptide conjugates. *Bioorg. Med. Chem. Lett.* **45**, 128122 (2021).
29. P. Sarkar, S. Samaddar, V. Ammanathan, V. Yarlagadda, C. Ghosh, M. Shukla, G. Kaul, R. Manjithaya, S. Chopra, J. Haldar, Vancomycin derivative inactivates carbapenem-resistant *Acinetobacter baumannii* and induces autophagy. *ACS Chem. Biol.* **15**, 884–889 (2020).
30. V. Yarlagadda, P. Akkapeddi, G. B. Manjunath, J. Haldar, Membrane active vancomycin analogues: A strategy to combat bacterial resistance. *J. Med. Chem.* **57**, 4558–4568 (2014).
31. V. Yarlagadda, S. Samaddar, K. Paramanandham, B. R. Shome, J. Haldar, Membrane disruption and enhanced inhibition of cell-wall biosynthesis: A synergistic approach to tackle vancomycin-resistant bacteria. *Angew. Chem. Int. Ed. Engl.* **54**, 13644–13649 (2015).
32. P. Sarkar, D. Basak, R. Mukherjee, J. E. Bandow, J. Haldar, Alkyl-aryl-vancomycins: Multimodal glycopeptides with weak dependence on the bacterial metabolic state. *J. Med. Chem.* **64**, 10185–10202 (2021).
33. M. A. T. Blaskovich, K. A. Hansford, Y. Gong, M. S. Butler, C. Muldoon, J. X. Huang, S. Ramu, A. B. Silva, M. Cheng, A. M. Kavanagh, Z. Ziora, R. Premraj, F. Lindahl, T. A. Bradford, J. C. Lee, T. Karoli, R. Pelingon, D. J. Edwards, M. Amado, A. G. Elliott, W. Phetsang, N. H. Daud, J. E. Deecke, H. E. Sidjabat, S. Ramaologa, J. Zuegg, J. R. Betley, A. P. G. Beevers, R. A. G. Smith, J. A. Roberts, D. L. Paterson, M. A. Cooper, Protein-inspired antibiotics active against vancomycin- and daptomycin-resistant bacteria. *Nat. Commun.* **9**, 22 (2018).
34. M. A. T. Blaskovich, K. A. Hansford, M. S. Butler, S. Ramu, A. M. Kavanagh, A. M. Jarrad, A. Prasetyoputri, M. E. Pitt, J. X. Huang, F. Lindahl, Z. M. Ziora, T. Bradford, C. Muldoon, P. Rajaratnam, R. Pelingon, D. J. Edwards, B. Zhang, M. Amado, A. G. Elliott, J. Zuegg, L. Coin, A.-K. Woischnig, N. Khanna, E. Breidenstein, A. Stincone, C. Mason, N. Khan, H.-K. Cho, M. J. Karau, K. E. Greenwood-Quaintance, R. Patel, M. Wootton, M. L. James, M. L. Hutton, D. Lyras, A. D. Ogunniyi, L. K. Mahdi, D. J. Trott, X. Wu, S. Niles, K. Lewis, J. R. Smith, K. E. Barber, J. Yim, S. A. Rice, M. J. Rybak, C. R. Ishmael, K. R. Hori, N. M. Bernthal, K. P. Francis, J. A. Roberts, D. L. Paterson, M. A. Cooper, A lipoglycopeptide antibiotic for Gram-positive biofilm-related infections. *Sci. Transl. Med.* **14**, eabj2381 (2022).
35. L. F. Neville, I. Shalit, P. A. Warn, M. H. Scheetz, J. Sun, M. B. Chosy, P. A. Wender, L. Cegelski, J. T. Rendell, In vivo targeting of *Escherichia coli* with vancomycin-arginine. *Antimicrob. Agents Chemother.* **65**, e02416–e02420 (2021).
36. F. Umstätter, C. Domhan, T. Hertlein, K. Ohlsen, E. Mühlberg, C. Kleist, S. Zimmermann, B. Beijer, K. D. Klika, U. Haberkorn, W. Mier, P. Uhl, Vancomycin resistance is overcome by conjugation of polycationic peptides. *Angew. Chem. Int. Ed. Engl.* **59**, 8823–8827 (2020).
37. A. Antonoplis, X. Zang, T. Wegner, P. A. Wender, L. Cegelski, Vancomycin-arginine conjugate inhibits growth of carbapenem-resistant *E. coli* and targets cell-wall synthesis. *ACS Chem. Biol.* **14**, 2065–2070 (2019).

38. Z.-C. Wu, M. D. Cameron, D. L. Boger, Vancomycin C-terminus guanidine modifications and further insights into an added mechanism of action imparted by a peripheral structural modification. *ACS Infect. Dis.* **6**, 2169–2180 (2020).
39. M. B. Chosy, J. Sun, H. P. Rahn, X. Liu, J. Brčić, P. A. Wender, L. Cegelski, Vancomycin-polyguanidino dendrimer conjugates inhibit growth of antibiotic-resistant Gram-positive and Gram-negative bacteria and eradicate biofilm-associated *S. aureus*. *ACS Infect. Dis.* **10**, 384–397 (2024).
40. A. Okano, N. A. Isley, D. L. Boger, Peripheral modifications of [Ψ[CH_2NH]Tpg^4]vancomycin with added synergistic mechanisms of action provide durable and potent antibiotics. *Proc. Natl. Acad. Sci. U.S.A.* **114**, 5052–5061 (2017).
41. J. Xie, J. G. Pierce, R. C. James, A. Okano, D. L. Boger, A redesigned vancomycin engineered for dual D-Ala-D-Ala and D-Ala-D-Lac binding exhibits potent antimicrobial activity against vancomycin-resistant bacteria. *J. Am. Chem. Soc.* **133**, 13946–13949 (2011).
42. A. Okano, A. Nakayama, K. Wu, E. A. Lindsey, A. W. Schammel, Y. Feng, K. C. Collins, D. L. Boger, Total syntheses and initial evaluation of [Ψ[C(=S)NH]Tpg^4]vancomycin, [Ψ[C(=NH)NH]Tpg^4]vancomycin, [Ψ[CH_2NH]Tpg^4]vancomycin, and their (4-chlorobiphenyl)methyl derivatives: Synergistic binding pocket and peripheral modifications for the glycopeptide antibiotics. *J. Am. Chem. Soc.* **137**, 3693–3704 (2015).
43. J. Xie, A. Okano, J. G. Pierce, R. C. James, S. Stamm, C. M. Crane, D. L. Boger, Total synthesis of [Ψ[C(=S)NH]Tpg^4]vancomycin glycon, [Ψ[C(=NH)NH]Tpg^4]vancomycin aglycon, and related key compounds: Reengineering vancomycin for dual D-Ala-D-Ala and D-Ala-D-Lac binding. *J. Am. Chem. Soc.* **134**, 1284–1297 (2012).
44. A. Okano, R. C. James, J. G. Pierce, J. Xie, D. L. Boger, Silver(I)-promoted conversion of thioamides to amidines: Divergent synthesis of a key series of vancomycin aglycon residue 4 amidines that clarify binding behavior to model ligands. *J. Am. Chem. Soc.* **134**, 8790–8793 (2012).
45. A. Okano, A. Nakayama, A. W. Schammel, D. L. Boger, Total synthesis of [Ψ[C(=NH)NH]Tpg^4]vancomycin and its (4-chlorobiphenyl)methyl derivative: Impact of peripheral modifications on vancomycin analogues redesigned for dual D-Ala-D-Ala and D-Ala- D-Lac binding. *J. Am. Chem. Soc.* **136**, 13522–13525 (2014).
46. B. M. Crowley, D. L. Boger, Total synthesis and evaluation of [Ψ[CH_2NH]Tpg^4]vancomycin aglycon: Reengineering vancomycin for dual D-Ala- D-Ala and D-Ala- D-Lac binding. *J. Am. Chem. Soc.* **128**, 2885–2892 (2006).
47. D. Guan, F. Chen, Y. Qiu, B. Jiang, L. Gong, L. Lan, W. Huang, Sulfonium, an underestimated moiety for structural modification, alters the antibacterial profile of vancomycin against multidrug-resistant bacteria. *Angew. Chem. Int. Ed. Engl.* **58**, 6678–6682 (2019).
48. M. J. Van Haren, N. Marechal, N. Troffer-Charlier, A. Cianciulli, G. Sbardella, J. Cavarelli, N. I. Martin, Transition state mimics are valuable mechanistic probes for structural studies with the arginine methyltransferase CARM1. *Proc. Natl. Acad. Sci. U.S.A.* **114**, 3625–3630 (2017).
49. C. A. Mooney, S. A. Johnson, P. T. Hart, L. Quarles Van Ufford, C. A. M. De Haan, E. E. Moret, N. I. Martin, Oseltamivir analogues bearing N-substituted guanidines as potent neuraminidase inhibitors. *J. Med. Chem.* **57**, 3154–3160 (2014).
50. A. Sevšek, J. Sastre Toraño, L. Quarles Van Ufford, E. E. Moret, R. J. Pieters, N. I. Martin, Orthoester functionalized *N*-guanidino derivatives of 1,5-dideoxy-1,5-imino-D-xylitol as pH-responsive inhibitors of β-glucocerebrosidase. *MedChemComm* **8**, 2050–2054 (2017).
51. Y. Zhang, M. J. van Haren, N. I. Martin, Peptidic transition state analogues as PRMT inhibitors. *Methods* **175**, 24–29 (2020).
52. Clinical and Laboratory Standards Institute (CLSI), *Performance Standards for Antimicrobial Susceptibility Testing* (CLSI guideline M100 ED32, 2022).
53. F. F. Arhin, I. Sarmiento, A. Belley, G. A. McKay, D. C. Draghi, P. Grover, D. F. Sahm, T. R. Parr, G. Moeck, Effect of polysorbate 80 on oritavancin binding to plastic surfaces: Implications for susceptibility testing. *Antimicrob. Agents Chemother.* **52**, 1597–1603 (2008).
54. A. Kavanagh, S. Ramu, Y. Gong, M. A. Cooper, M. A. T. Blaskovich, Effects of microplate type and broth additives on microdilution MIC susceptibility assays. *Antimicrob. Agents Chemother.* **63**, e01760-18 (2021).
55. K. Wanat, Biological barriers, and the influence of protein binding on the passage of drugs across them. *Mol. Biol. Rep.* **47**, 3221–3231 (2020).
56. B. L. Lee, M. Sachdeva, H. F. Chambers, Effect of protein binding of daptomycin on MIC and antibacterial activity. *Antimicrob. Agents Chemother.* **35**, 2505–2508 (1991).
57. R. D. Plaut, C. P. Mocca, R. Prabhakara, T. J. Merkel, S. Stibitz, Stably luminescent *Staphylococcus aureus* clinical strains for use in bioluminescent imaging. *PLOS ONE* **8**, e59232 (2013).
58. H. Liu, N. K. Archer, C. A. Dillen, Y. Wang, A. G. Ashbaugh, R. V. Ortines, T. Kao, S. K. Lee, S. S. Cai, R. J. Miller, M. C. Marchitto, E. Zhang, D. P. Riggins, R. D. Plaut, S. Stibitz, R. S. Geha, L. S. Miller, *Staphylococcus aureus* epicutaneous exposure drives skin inflammation via IL-36-mediated T cell responses. *Cell Host Microbe* **22**, 653–666.e5 (2017).
59. R. R. Regoes, C. Wiuff, R. M. Zappala, K. N. Garner, F. Baquero, B. R. Levin, Pharmacodynamic functions: A multiparameter approach to the design of antibiotic treatment regimens. *Antimicrob. Agents Chemother.* **48**, 3670–3676 (2004).
60. A. J. O'Neill, I. Chopra, Preclinical evaluation of novel antibacterial agents by microbiological and molecular techniques. *Expert Opin. Investig. Drugs* **13**, 1045–1063 (2004).
61. J. L. Lister, A. R. Horswill, *Staphylococcus aureus* biofilms: Recent developments in biofilm dispersal. *Front. Cell. Infect. Microbiol.* **4**, 178 (2014).
62. C. J. Sanchez, K. Mende, M. L. Beckius, K. S. Akers, D. R. Romano, J. C. Wenke, C. K. Murray, Biofilm formation by clinical isolates and the implications in chronic infections. *BMC Infect. Dis.* **13**, 47 (2013).
63. E. G. Di Domenico, S. G. Rimoldi, I. Cavallo, G. D'Agosto, E. Trento, G. Cagnoni, A. Palazzin, C. Pagani, F. Romeri, E. De Vecchi, M. Schiavini, D. Secchi, C. Antona, G. Rizzardini, R. B. Dichirico, L. Toma, D. Kovacs, G. Cardinali, M. T. Gallo, M. R. Gismondo, F. Ensoli, Microbial biofilm correlates with an increased antibiotic tolerance and poor therapeutic outcome in infective endocarditis. *BMC Microbiol.* **19**, 228 (2019).
64. D. Rodríguez-Lázaro, C. Alonso-Calleja, E. A. Oniciuc, R. Capita, D. Gallego, C. González-Machado, M. Wagner, V. Barbu, J. M. Eiros-Bouza, A. I. Nicolau, M. Hernández, Characterization of biofilms formed by foodborne methicillin-resistant *Staphylococcus aureus*. *Front. Microbiol.* **9**, 3004 (2018).
65. P. E. Reynolds, Studies on the mode of action of vancomycin. *Biochim. Biophys. Acta* **52**, 403–405 (1961).
66. E. A. Somner, P. E. Reynolds, Inhibition of peptidoglycan biosynthesis by ramoplanin. *Antimicrob. Agents Chemother.* **34**, 413–419 (1990).
67. G. Siewert, J. L. Strominger, Bacitracin: An inhibitor of the dephosphorylation of lipid pyrophosphate, an intermediate in the biosynthesis of the peptidoglycan of bacterial cell walls. *Proc. Natl. Acad. Sci. U.S.A.* **57**, 767–773 (1967).
68. H. Strahl, L. W. Hamoen, Membrane potential is important for bacterial cell division. *Proc. Natl. Acad. Sci. U.S.A.* **107**, 12281–12286 (2010).
69. D. A. Beauregard, D. H. Williams, M. N. Gwynn, D. J. C. Knowles, Dimerization and membrane anchors in extracellular targeting of vancomycin group antibiotics. *Antimicrob. Agents Chemother.* **39**, 781–785 (1995).
70. D. Kahne, C. Leimkuhler, W. Lu, C. Walsh, Glycopeptide and lipoglycopeptide antibiotics. *Chem. Rev.* **105**, 425–448 (2005).
71. J. G. Hurdle, A. J. O'Neill, I. Chopra, R. E. Lee, Targeting bacterial membrane function: An underexploited mechanism for treating persistent infections. *Nat. Rev. Microbiol.* **9**, 62–75 (2011).
72. F. Van Bambeke, Lipoglycopeptide antibacterial agents in Gram-positive infections: A comparative review. *Drugs* **75**, 2073–2095 (2015).
73. P. Jay Sims, A. S. Waggoner, C.-H. Wang, J. F. Hoffman, Studies on the mechanism by which cyanine dyes measure membrane potential in red blood cells and phosphatidylcholine vesicles. *Biochemistry* **13**, 3315–3330 (1974).
74. A. Belley, G. A. McKay, F. F. Arhin, I. Sarmiento, S. Beaulieu, I. Fadhil, T. R. Parr, G. Moeck, Oritavancin disrupts membrane integrity of *Staphylococcus aureus* and vancomycin-resistant enterococci to effect rapid bacterial killing. *Antimicrob. Agents Chemother.* **54**, 5369–5371 (2010).
75. A. Belley, E. Neesham-Grenon, G. McKay, F. F. Arhin, R. Harris, T. Beveridge, T. R. Parr, G. Moeck, Oritavancin kills stationary-phase and biofilm *Staphylococcus aureus* cells in vitro. *Antimicrob. Agents Chemother.* **53**, 918–925 (2009).
76. D. J. Arndt-Jovin, T. M. Jovin, Chapter 16 fluorescence labeling and microscopy of DNA. *Methods Cell Biol.* **30**, 417–448 (1989).
77. M. Lázaro-Díez, S. Remuzgo-Martínez, C. Rodríguez-Mirones, F. Acosta, J. M. Icardo, L. Martínez-Martínez, J. Ramos-Vivas, Effects of subinhibitory concentrations of ceftaroline on methicillin-resistant *Staphylococcus aureus* (MRSA) biofilms. *PLOS ONE* **11**, e0147569 (2016).
78. E. Breukink, B. de Kruijff, Lipid II as a target for antibiotics. *Nat. Rev. Drug Discov.* **5**, 321–323 (2006).
79. J. P. Mackay, U. Gerhard, D. A. Beauregard, D. H. Williams, M. S. Westwell, M. S. Searle, Glycopeptide antibiotic activity and the possible role of dimerization: A model for biological signaling. *J. Am. Chem. Soc.* **116**, 4581–4590 (1994).
80. T. Mascher, S. L. Zimmer, T.-A. Smith, J. D. Helmann, Antibiotic-inducible promoter regulated by the cell envelope stress-sensing two-component system LiaRS of *Bacillus subtilis*. *Antimicrob. Agents Chemother.* **48**, 2888–2896 (2004).
81. J. Radeck, S. Gebhard, P. S. Orchard, M. Kirchner, S. Bauer, T. Mascher, G. Fritz, Anatomy of the bacitracin resistance network in *Bacillus subtilis*. *Mol. Microbiol.* **100**, 607–620 (2016).
82. S. Tan, K. C. Ludwig, A. Müller, T. Schneider, J. R. Nodwell, The lasso peptide siamycin-I targets lipid II at the Gram-positive cell surface. *ACS Chem. Biol.* **14**, 966–974 (2019).
83. D. Münch, I. Engels, A. Müller, K. Reder-Christ, H. Falkenstein-Paul, G. Bierbaum, F. Grein, G. Bendas, H.-G. Sahl, T. Schneider, Structural variations of the cell wall precursor lipid II and their influence on binding and activity of the lipoglycopeptide antibiotic oritavancin. *Antimicrob. Agents Chemother.* **59**, 772–781 (2015).
84. D. Münch, T. Roemer, S. H. Lee, M. Engeser, H. G. Sahl, T. Schneider, Identification and in vitro analysis of the GatD/MurT enzyme-complex catalyzing lipid II amidation in *Staphylococcus aureus*. *PLOS Pathog.* **8**, e1002509 (2012).

85. S. Gudmundsson, H. Erlendsdóttir, "Murine thigh infection model" in *Handbook of Animal Models of Infection*, O. Zak, M. A. Sande, Eds. (Academic Press, Elsevier, 1999), pp. 137–144.
86. F. A. Groothuis, N. Timmer, E. Opsahl, B. Nicol, S. T. J. Droge, B. J. Blaauboer, N. I. Kramer, Influence of in vitro assay setup on the apparent cytotoxic potency of benzalkonium chlorides. *Chem. Res. Toxicol.* **32**, 1103–1114 (2019).
87. L. Urban, S. Whitebread, J. Hamon, D. Mikhailov, K. Azzaoui, "Screening for safety—relevant off-target activities" in *Polypharmacology in Drug Discovery.* (Wiley, 2012), pp. 15–46.
88. R. Nau, F. Sörgel, H. Eiffert, Penetration of drugs through the blood-cerebrospinal fluid/blood-brain barrier for treatment of central nervous system infections. *Clin. Microbiol. Rev.* **23**, 858–883 (2010).
89. S. Barriere, F. Genter, E. Spencer, M. Kitt, D. Hoelscher, J. Morganroth, Effects of a new antibacterial, telavancin, on cardiac repolarization (QTc interval duration) in healthy subjects. *J. Clin. Pharmacol.* **44**, 689–695 (2004).
90. B. Darpo, S. K. Lee, T. E. Moon, N. Sills, J. W. Mason, Oritavancin, a new lipoglycopeptide antibiotic: Results from a thorough QT study. *J. Clin. Pharmacol.* **50**, 895–903 (2010).
91. European Medicines Agency (EMA), Committee for Medicinal Products for Human Use (CHMP), *Assessment report Orbactiv, INN-oritavancin* (EMA/CHMP/803704/2015, 2015); https://ema.europa.eu/en/documents/assessment-report/tenkasi-previously-orbactiv-epar-public-assessment-report_en.pdf.
92. J. Beer, C. C. Wagner, M. Zeitlinger, Protein binding of antimicrobials: Methods for quantification and for investigation of its impact on bacterial killing. *AAPS J.* **11**, 1–12 (2009).
93. G. M. Pais, J. Liu, S. Zepcan, S. N. Avedissian, N. J. Rhodes, K. J. Downes, G. S. Moorthy, M. H. Scheetz, Vancomycin-induced kidney injury: Animal models of toxicodynamics, mechanisms of injury, human translation, and potential strategies for prevention. *Pharmacotherapy* **40**, 438–454 (2020).
94. D. P. Levine, Vancomycin: A history. *Clin. Infect. Dis.* **42**, S5–S12 (2006).
95. D. J. Greenblatt, E. M. Sellers, J. Koch-Weser, Importance of protein binding for the interpretation of serum or plasma drug concentrations. *J. Clin. Pharmacol.* **22**, 259–263 (1982).
96. D. J. Merrikin, J. Briant, G. N. Rolinson, Effect of protein binding on antibiotic activity in vivo. *J. Antimicrob. Chemother.* **11**, 233–238 (1983).
97. S. Schmidt, K. Röck, M. Sahre, O. Burkhardt, M. Brunner, M. T. Lobmeyer, H. Derendorf, Effect of protein binding on the pharmacological activity of highly bound antibiotics. *Antimicrob. Agents Chemother.* **52**, 3994–4000 (2008).
98. F. F. Arhin, A. Belley, G. McKay, S. Beaulieu, I. Sarmiento, T. R. Parr Jr., G. Moeck, Assessment of oritavancin serum protein binding across species. *Antimicrob. Agents Chemother.* **54**, 3481–3483 (2010).
99. D. J. Payne, M. N. Gwynn, D. J. Holmes, D. L. Pompliano, Drugs for bad bugs: Confronting the challenges of antibacterial discovery. *Nat. Rev. Drug Discov.* **6**, 29–40 (2007).
100. E. M. Bailey, M. J. Rybak, G. W. Kaatz, Comparative effect of protein binding on the killing activities of teicoplanin and vancomycin. *Antimicrob. Agents Chemother.* **35**, 1089–1092 (1991).
101. A. Belley, D. L. Seguin, F. Arhin, G. Moeck, Comparative in vitro activities of oritavancin, dalbavancin, and vancomycin against methicillin-resistant *Staphylococcus aureus* isolates in a nondividing state. *Antimicrob. Agents Chemother.* **60**, 4342–4345 (2016).
102. A. J. Lepak, M. Zhao, D. R. Andes, Comparative pharmacodynamics of telavancin and vancomycin in the neutropenic murine thigh and lung infection models against *Staphylococcus aureus*. *Antimicrob. Agents Chemother.* **61**, e00281–17 (2017).
103. D. Andes, W. A. Craig, In vivo pharmacodynamic activity of the glycopeptide dalbavancin. *Antimicrob. Agents Chemother.* **51**, 1633–1642 (2007).
104. C. J. Boylan, K. Campanale, P. W. Iversen, D. L. Phillips, M. L. Zeckel, T. R. Parr, Pharmacodynamics of oritavancin (LY333328) in a neutropenic-mouse thigh model of *Staphylococcus aureus* infection. *Antimicrob. Agents Chemother.* **47**, 1700–1706 (2003).
105. C. E. Pollard, M. Skinner, S. E. Lazic, H. M. Prior, K. M. Conlon, J.-P. Valentin, C. Dota, An analysis of the relationship between preclinical and clinical QT interval-related data. *Toxicol. Sci.* **159**, 94–101 (2017).
106. L. L. Vincent, C. M. Otto, Infective endocarditis: Update on epidemiology, outcomes, and management. *Curr. Cardiol. Rep.* **20**, 86 (2018).
107. L. Ajaka, E. Heil, S. Schmalzle, Dalbavancin in the treatment of bacteremia and endocarditis in people with barriers to standard care. *Antibiotics* **9**, 700 (2020).
108. E. Durante-Mangoni, F. Boccia, M. P. Ursi, A. Karruli, R. Andini, M. Galdo, R. Zampino, Dalbavancin for infective endocarditis: A single centre experience. *J. Chemother.* **33**, 256–262 (2021).
109. J. M. Steele, R. W. Seabury, C. M. Hale, B. T. Mogle, Unsuccessful treatment of methicillin-resistant *Staphylococcus aureus* endocarditis with dalbavancin. *J. Clin. Pharm. Ther.* **43**, 101–103 (2018).
110. M. Kussmann, M. Karer, M. Obermueller, K. Schmidt, W. Barousch, D. Moser, M. Nehr, M. Ramharter, W. Poeppl, A. Makristathis, S. Winkler, F. Thalhammer, H. Burgmann, H. Lagler, Emergence of a dalbavancin induced glycopeptide/lipoglycopeptide non-susceptible *Staphylococcus aureus* during treatment of a cardiac device-related endocarditis. *Emerg. Microbes Infect.* **7**, 202 (2018).
111. E. J. Filippone, W. K. Kraft, J. L. Farber, The nephrotoxicity of vancomycin. *Clin. Pharmacol. Ther.* **102**, 459–469 (2017).
112. National Academies Press, *Guide for the Care and Use of Laboratory Animals, 8th edition* (2011); https://grants.nih.gov/grants/olaw/guide-for-the-care-and-use-of-laboratory-animals.pdf.
113. T. Koopmans, T. M. Wood, P. 't Hart, L. H. J. Kleijn, A. P. A. Hendrickx, R. J. L. Willems, E. Breukink, N. I. Martin, Semisynthetic lipopeptides derived from nisin display antibacterial activity and lipid II binding on par with that of the parent compound. *J. Am. Chem. Soc.* **137**, 9382–9389 (2015).
114. G. M. Coppola, M. Prashad, A convenient preparation of farnesylamine. *Synth. Commun.* **23**, 535–541 (1993).
115. T. J. Zahn, M. Eilers, Z. Guo, M. B. Ksebati, M. Simon, J. D. Scholten, S. O. Smith, R. A. Gibbs, Evaluation of isoprenoid conformation in solution and in the active site of protein-farnesyl transferase using carbon-13 labeling in conjunction with solution- and solid-state NMR. *J. Am. Chem. Soc.* **122**, 7153–7164 (2000).
116. H. Xie, Y. Shao, J. M. Becker, F. Naider, R. A. Gibbs, Synthesis and biological evaluation of the geometric farnesylated analogues of the a-factor mating peptide of *Saccharomyces cerevisiae*. *J. Org. Chem.* **65**, 8552–8563 (2000).
117. H. Lee, K. D. Park, X.-F. Yang, E. T. Dustrude, S. M. Wilson, R. Khanna, H. Kohn, (Biphenyl-4-yl)methylammonium chlorides: Potent anticonvulsants that modulate Na^+ currents. *J. Med. Chem.* **56**, 5931–5939 (2013).
118. N. I. Martin, J. J. Woodward, M. A. Marietta, N^G-hydroxyguanidines from primary amines. *Org. Lett.* **8**, 4035–4038 (2006).
119. A. Hughes, D. Byun, Y. Chen, M. Fleury, J. R. Jacobsen, E. Stangeland, R. D. Wilson, R. Yen, Patent WO2010123766A1 (2010).
120. C. M. Pearce, D. H. Williams, Complete assignment of the ^{13}C NMR spectrum of vancomycin. *J. Chem. Soc. Perkin Trans. 2*, 153–157 (1995).
121. A. Müller, D. Münch, Y. Schmidt, K. Reder-Christ, G. Schiffer, G. Bendas, H. Gross, H.-G. Sahl, T. Schneider, H. Brötz-Oesterhelt, Lipodepsipeptide empedopeptin inhibits cell wall biosynthesis through Ca^{2+}-dependent complex formation with peptidoglycan precursors. *J. Biol. Chem.* **287**, 20270–20280 (2012).
122. T. Schneider, M. M. Senn, B. Berger-Bächi, A. Tossi, H. G. Sahl, I. Wiedemann, In vitro assembly of a complete, pentaglycine interpeptide bridge containing cell wall precursor (lipid II-Gly_5) of *Staphylococcus aureus*. *Mol. Microbiol.* **53**, 675–685 (2004).
123. L. L. Ling, T. Schneider, A. J. Peoples, A. L. Spoering, I. Engels, B. P. Conlon, A. Mueller, T. F. Schäberle, D. E. Hughes, S. Epstein, M. Jones, L. Lazarides, V. A. Steadman, D. R. Cohen, C. R. Felix, K. A. Fetterman, W. P. Millett, A. G. Nitti, A. M. Zullo, C. Chen, K. Lewis, A new antibiotic kills pathogens without detectable resistance. *Nature* **517**, 455–459 (2015).
124. Y. Imai, K. J. Meyer, A. Iinishi, Q. Favre-Godal, R. Green, S. Manuse, M. Caboni, M. Mori, S. Niles, M. Ghiglieri, C. Honrao, X. Ma, J. J. Guo, A. Makriyannis, L. Linares-Otoya, N. Böhringer, Z. G. Wuisan, H. Kaur, R. Wu, A. Mateus, A. Typas, M. M. Savitski, J. L. Espinoza, A. O'Rourke, K. E. Nelson, S. Hiller, N. Noinaj, T. F. Schäberle, A. D'Onofrio, K. Lewis, A new antibiotic selectively kills Gram-negative pathogens. *Nature* **576**, 459–464 (2019).
125. Innovotech, "The MBEC Physiology and Genetics assay: Instruction manual" (2008).
126. T. Schneider, T. Kruse, R. Wimmer, I. Wiedemann, V. Sass, U. Pag, A. Jansen, A. K. Nielsen, P. H. Mygind, D. S. Raventós, S. Neve, B. Ravn, A. M. J. J. Bonvin, L. De Maria, A. S. Andersen, L. K. Gammelgaard, H. G. Sahl, H. H. Kristensen, Plectasin, a fungal defensin, targets the bacterial cell wall precursor lipid II. *Science* **328**, 1168–1172 (2010).
127. A. Müller, M. Wenzel, H. Strahl, F. Grein, T. N. V. Saaki, B. Kohl, T. Siersma, J. E. Bandow, H. G. Sahl, T. Schneider, L. W. Hamoen, Daptomycin inhibits cell envelope synthesis by interfering with fluid membrane microdomains. *Proc. Natl. Acad. Sci. U.S.A.* **113**, E7077–E7086 (2016).
128. F. Grein, A. Müller, K. M. Scherer, X. Liu, K. C. Ludwig, A. Klöckner, M. Strach, H. G. Sahl, U. Kubitscheck, T. Schneider, Ca^{2+}-daptomycin targets cell wall biosynthesis by forming a tripartite complex with undecaprenyl-coupled intermediates and membrane lipids. *Nat. Commun.* **11**, 1455 (2020).
129. P. D. Rick, G. L. Hubbard, M. Kitaoka, H. Nagaki, T. Kinoshita, S. Dowd, V. Simplaceanu, C. Ho, Characterization of the lipid-carrier involved in the synthesis of enterobacterial common antigen (ECA) and identification of a novel phosphoglyceride in a mutant of *Salmonella typhimurium* defective in ECA synthesis. *Glycobiology* **8**, 557–567 (1998).
130. G. de Aragão Umbuzeiro, C. M. Rech, S. Correia, A. M. Bergamasco, G. H. L. Cardenette, S. Flückiger-Isler, M. Kamber, Comparison of the Salmonella/microsome microsuspension assay with the new microplate fluctuation protocol for testing the mutagenicity of environmental samples. *Environ. Mol. Mutagen.* **51**, 31–38 (2010).

131. R. Corvi, S. Albertini, T. Hartung, S. Hoffmann, D. Maurici, S. Pfuhler, J. van Benthem, P. Vanparys, ECVAM retrospective validation of in vitro micronucleus test (MNT). *Mutagenesis* **23**, 271–283 (2008).
132. D. K. Grandy, M. A. Marchionni, H. Makam, R. E. Stofko, M. Alfano, L. Frothingham, J. B. Fischer, K. J. Burke-Howie, J. R. Bunzow, A. C. Server, Cloning of the cDNA and gene for a human D_2 dopamine receptor. *Proc. Natl. Acad. Sci. U.S.A.* **86**, 9762–9766 (1989).
133. T. Pacholczyk, R. D. Blakely, S. G. Amara, Expression cloning of a cocaine-and antidepressant-sensitive human noradrenaline transporter. *Nature* **350**, 350–354 (1991).
134. F. Simonin, C. Gavériaux-Ruff, K. Befort, H. Matthes, B. Lannes, G. Micheletti, M. G. Mattéi, G. Charron, B. Bloch, B. Kieffer, kappa-Opioid receptor in humans: cDNA and genomic cloning, chromosomal assignment, functional expression, pharmacology, and expression pattern in the central nervous system. *Proc. Natl. Acad. Sci. U.S.A.* **92**, 7006–7010 (1995).
135. D.-S. Choi, G. Birraux, J.-M. Launay, L. Maroteaux, The human serotonin 5-HT2B receptor: Pharmacological link between 5-HT2 and 5-HT1D receptors. *FEBS Lett.* **352**, 393–399 (1994).
136. R. C. Elkins, M. R. Davies, S. J. Brough, D. J. Gavaghan, Y. Cui, N. Abi-Gerges, G. R. Mirams, Variability in high-throughput ion-channel screening data and consequences for cardiac safety assessment. *J. Pharmacol. Toxicol. Methods* **68**, 112–122 (2013).
137. K. P. Bateman, J. Castro-Perez, M. Wrona, J. P. Shockcor, K. Yu, R. Oballa, D. A. Nicoll-Griffith, MS^E with mass defect filtering for in vitro and in vivo metabolite identification. *Rapid Commun. Mass Spectrom.* **21**, 1485–1496 (2007).
138. L. Di, E. H. Kerns, Y. Hong, H. Chen, Development and application of high throughput plasma stability assay for drug discovery. *Int. J. Pharm.* **297**, 110–119 (2005).
139. R. S. Obach, J. G. Baxter, T. E. Liston, B. M. Silber, B. C. Jones, F. Macintyre, D. J. Rance, P. Wastall, The prediction of human pharmacokinetic parameters from preclinical and in vitro metabolism data. *J. Pharmacol. Exp. Ther.* **283**, 46–58 (1997).
140. M. J. Banker, T. H. Clark, J. A. Williams, Development and validation of a 96-well equilibrium dialysis apparatus for measuring plasma protein binding. *J. Pharm. Sci.* **92**, 967–974 (2003).
141. European Medicines Agency (EMA), *Public Assessment Report Vibativ, INN: telavancin* (Procedure No.: EMEA/H/C/1240, 2011); https://ema.europa.eu/en/documents/assessment-report/vibativ-epar-public-assessment-report_en.pdf.
142. E. N. Fisher, E. S. Melnikov, V. Gegeckori, N. V. Potoldykova, D. V. Enikeev, K. A. Pavlenko, S. Agatonovic-Kustrin, D. W. Morton, G. V. Ramenskaya, Development and validation of an LC-MS/MS method for simultaneous determination of short peptide-based drugs in human blood plasma. *Molecules* **27**, 7831 (2022).

Acknowledgments: We thank P. Innocenti for the HR-MS recording and analysis, M. Nardella for the recording of 2D NMR spectra, and E. Fujichima Casara for measuring MIC values in the absence of P80. We thank S. Tandar, A. Koumans, and L. Baars for support with luminescence-based time-kill assays and R. Plaut for sharing the SAP229 and SAP430 *S. aureus* strains. A. Peters, A.-M. Salisbury, and S. Roychowdhury are thanked for productive input. **Funding:** Financial support was provided by the European Research Council (ERC consolidator grant to N.I.M., grant agreement no. 725523), Netherlands Scientific Organization (NWO NACTAR project number 18504), and the German Research Foundation (DFG, Project-ID 398967434–TRR 261). **Author contributions:** N.I.M., E.G., K.H.M.E.T., and N.W. designed the original project. E.G., E.M., V.L., F.M.S., and J.T.Z. synthesized and purified compounds. E.G., E.M., I.K., M.A., A.B., S.D.B., P.C., J.G., W.K.S., J.W., and J.G.C.H. performed biochemical or cell-based experiments and analyzed the results. K.H. conducted animal studies at Evotec UK. N.I.M., P.S.G., C.A.H., E.G., and E.M. managed, oversaw, and coordinated the project. N.I.M., T.S., D.-J.S., and M.S. supervised the experimental work. E.G. and N.I.M. wrote the original manuscript draft, and E.M. and N.I.M. wrote the revised manuscript. **Competing interests:** N.I.M., E.G., K.H.M.E.T., and N.W. are listed as inventors on a patent application filing WO2021060980A1; title: "Antibiotic compounds"; priority date: 24 September 2019, which includes compounds described in this article. K.H. is an employee of Evotec Ltd. (UK), a contract research organization active in antimicrobial research. P.S.G. and C.A.H. are independent paid pharmaceutical consultants for pharmaceutical and biotechnology companies and academic institutions on subject areas not related to this study. All other authors declare that they have no competing interests. **Data and materials availability:** All data associated with this study are present in the paper or the Supplementary Materials. Samples of compounds reported are available upon request, depending on available supply and under condition of a signed material transfer agreement. Data from figures are in data file S1.

Submitted 5 February 2022
Resubmitted 23 February 2024
Accepted 16 July 2024
Published 7 August 2024
10.1126/scitranslmed.abo4736